

The Holographic Dual of Strongly γ -deformed $N=4$ SYM Theory: Derivation, Generalization, Integrability and Discrete Reparametrization Symmetry

Nikolay Gromov^{a,b} **Amit Sever**^{c,d}

^a*Mathematics Department, King's College London, The Strand, London WC2R 2LS, UK*

^b*St.Petersburg INP, Gatchina, 188 300, St.Petersburg, Russia*

^c*School of Physics and Astronomy, Tel Aviv University, Ramat Aviv 69978, Israel*

^d*CERN, Theoretical Physics Department, 1211 Geneva 23, Switzerland*

E-mail: nikolay.gromov@kcl.ac.uk, amit.sever@cern.ch

ABSTRACT: Recently, we constructed the first-principle derivation of the holographic dual of $\mathcal{N} = 4$ SYM in the double-scaled γ -deformed limit directly from the CFT side. The dual fishchain model is a novel integrable chain of particles in AdS_5 . It can be viewed as a discretized string and revives earlier string-bit approaches. The original derivation was restricted to the operators built out of one of two types of scalar fields. In this paper, we extend our results to the general operators having any number of scalars of both types, except for a very special case when their numbers are equal. Interestingly, the extended model reveals a new discrete reparametrization symmetry of the “world-sheet”, preserving all integrals of motion. We use integrability to formulate a closed system of equations, which allows us to solve for the spectrum of the model in full generality, and present non-perturbative numerical results. We show that our results are in agreement with the Asymptotic Bethe Ansatz of the fishnet model up to the wrapping order at weak coupling.

Contents

1	Introduction	2
2	Notations and set-up	3
2.1	Fishnet model	3
2.2	Fishchain model	5
3	CFT wave function and the graph building operator	7
3.1	Inverting the graph building operator	9
3.2	Quantum fishchain with magnons	12
3.3	Adding anti-magnons to the QFC	13
4	Integrability of the fishchain with magnons	14
5	Discrete reparametrization symmetry	17
5.1	Cutting and leveling	18
5.2	The cut deformation operators	19
5.3	The fishchain reparametrization operators	20
6	Integrability, Exact Spectrum and Reparametrization Invariance	21
6.1	T-functions and Baxter TQ relation	22
6.2	Discrete reparametrization symmetry and integrability	24
6.3	Quantization condition and exact spectrum	26
6.4	Numerical tests	26
6.4.1	Length three, one magnon	27
6.4.2	Length three, two magnons	28
7	Conclusion	28

1 Introduction

The strongly γ -deformed limit of $\mathcal{N} = 4$ SYM, also known as the *fishnet model* [1–3], is an ideal playground for developing our exact computational methods and understanding holography. It is an interacting four-dimensional QFT with $SU(N)$ symmetry that one could hope is solvable exactly in the planar limit. Just like the planar limit of $\mathcal{N} = 4$ SYM theory, this model is conformal for any value of the 't Hooft coupling ξ . It consists of two complex $N \times N$ matrix scalars ϕ_1 and ϕ_2 that are weakly coupled when $\xi \rightarrow 0$. At strong coupling $\xi \rightarrow \infty$, a new classical dual description emerges in terms of a chain of scalars in AdS_5 [4]. At finite ξ the theory becomes rather complicated. At the same time, it is much simpler than $\mathcal{N} = 4$ SYM. For example, at each order of the perturbation theory, there are only very few Feynman diagrams that contribute.

There are several properties that make the fishnet theory particularly interesting and tractable. First, the model can be proven to be integrable at the quantum level [1–3]. Second, its Holographic dual fishchain theory can be derived rigorously and quantized exactly [4, 5]. This contrasts with the current status of $\mathcal{N} = 4$ theory, where the integrability is conjectured and the dual super-string in $AdS_5 \times S^5$ can only be quantized semi-classically.

So far, our derivation and quantization of the fishchain model was restricted to a set of states/operators that belong to the so-called $\mathfrak{u}(1)$ sector. These are operators of the type $\mathcal{O} = \text{tr} [\phi_1^J \partial^m (\phi_2 \phi_2^\dagger)^n \dots]$, which can carry arbitrary spin and are only charged under the $\mathfrak{u}(1)_1$ subgroup of the total $\mathfrak{u}(1)_1 \times \mathfrak{u}(1)_2$ symmetry that rotates the two types of scalars. The main objective of this paper is to extend the derivation to general states, carrying both quantum numbers. This involves introduction of the *magnons* i.e. ϕ_2 fields in the background of J ϕ_1 's. While most of the steps go through very similar to our previous work, we find that the inclusion of the magnons leads naturally to a new notion of a *discrete reparametrization gauge symmetry*. It is the string-bit counterpart of the smooth string reparametrization freedom, which relates different ways of parametrizing the same state.¹ Furthermore, extending the integrability construction to all operators allows us, in particular, to solve the spectrum with magnons included, which is a new result by itself. The solution takes the form of a Baxter TQ-relations, subjected to the quantization conditions of [7] and generalizing results of [8]. It allows us to compute the conformal dimension of almost all single trace operators². Moreover, this construction gives the general framework for development of the integrability based separation of variables method (SoV) for more general observables such as correlation functions.

The paper is organized as follows. In section 2 we introduce our notations and review the main previous results, which are important for this paper. In particular, we recall the main steps from [5] for the quantization procedure of the fishchain. In section 3, we generalize the notion of the CFT wave function, initially introduced in [5], to operators with magnons. We then construct the corresponding graph building operator and derive its holographic counterpart. In section 4, we establish the integrability of the fishchain model

¹This symmetry is reminiscent of the Yangian symmetry of planar scattering amplitudes studied in [6].

²There are some additional technical difficulties in deriving the spectrum for a special case when both $U(1)$ charges are equal.

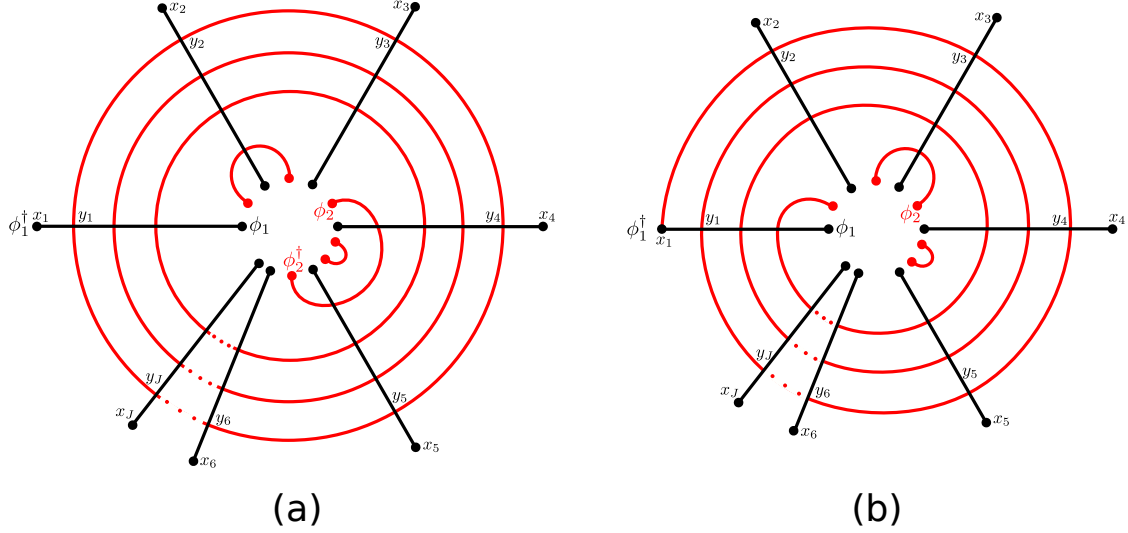


Figure 1. a) Feynman diagrams that contribute to the correlation function of an operator of the form $\text{tr}(\partial^m \phi_1^J (\phi_2 \phi_2^\dagger)^n \dots)$ are all of fishnet type – made of the iterative wheel as shown on the diagram [2]. This structure can be resummed and leads to integrability [3]. b) For operators with also net ϕ_2 charge, (2.3), the diagrams are of iterative spider type [9].

with magnons. In section 5, we identify redundancy in the space of CFT wave functions that we associate to a discrete reparametrization symmetry of the fishchain model. In section 6, we solve the spectrum of the model with magnons and prove its reparametrization symmetry. We conclude in the section 7.

2 Notations and set-up

Here, we introduce the notations and give a short introduction to our results from [4, 5].

2.1 Fishnet model

The *fishnet model* [1] is defined by the following action³

$$\mathcal{L}_{4d} = N \text{tr} \left(|\partial \phi_1|^2 + |\partial \phi_2|^2 + (4\pi)^2 \xi^2 \phi_1^\dagger \phi_2^\dagger \phi_1 \phi_2 \right). \quad (2.1)$$

This model was obtained in [1] by taking a double scaling limit of γ -deformed $\mathcal{N} = 4$ SYM theory. Hence, we will still impose the Gauss constraint and will only consider operators that are neutral under the $SU(N)$ part of the global symmetries.

Our previous consideration was restricted to a subset of all operators, known as the $\mathfrak{u}(1)$ sector

$$\mathcal{O}_J = \text{tr} [\partial^m \phi_1^J (\phi_2 \phi_2^\dagger)^n \dots] + \dots \quad (2.2)$$

containing any number of derivatives, J -scalar fields ϕ_1 and any *neutral* combination of ϕ_2 and ϕ_2^\dagger . Correlation functions of $\mathfrak{u}(1)$ operators are given by the sum of fishnet type

³We have suppressed double trace interactions which are not relevant non-perturbatively [11–13].

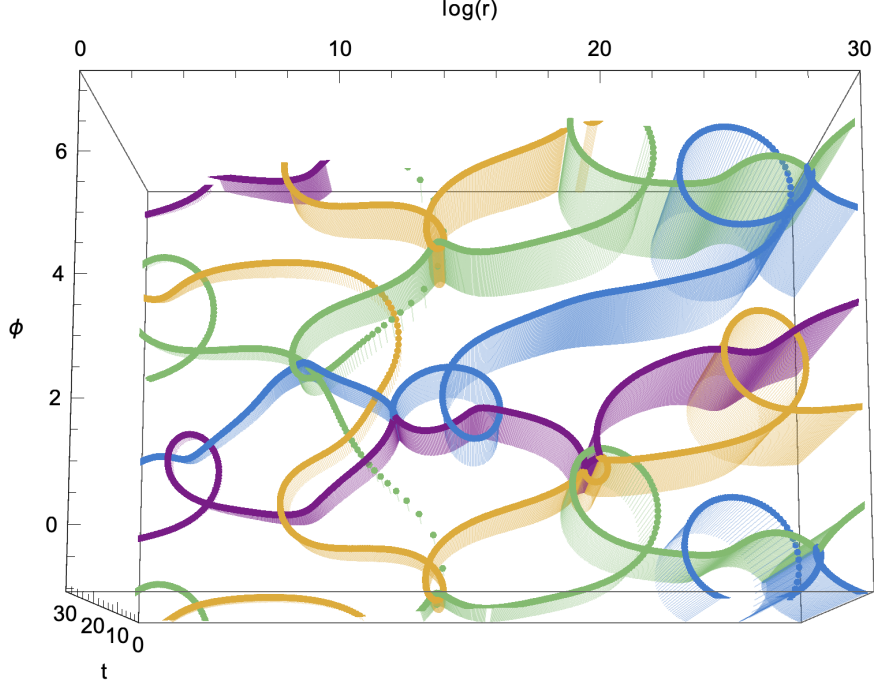


Figure 2. Dynamics of the fishchain consisting of $J = 4$ particles (denoted by different colours). The initial conditions are restricted to a 2D plane after projection on the boundary. The plane is parametrized in the radial parameters by the angle ϕ and the radius r . The third axis corresponds to the time. The drift in ϕ is due to a non-zero total angular momentum S and the exponential expansion in r is due to $\Delta > 0$.

diagrams. These are diagrams that are made of the iterative wheel structure as is demonstrated in figure 1.a.

General single trace operators in the model can also carry $u(1)_2$ charge. They take the schematic form

$$\mathcal{O}_{J_1} = \text{tr} [\partial^{m_1} \phi_1^{J_1} \partial^{m_2} \phi_2^{J_2} (\phi_2 \phi_2^\dagger)^{n_1} (\phi_1^\dagger \phi_1)^{n_2} \dots] + \dots \quad (2.3)$$

In this paper we allow for arbitrary values of J_1 and J_2 as long as $|J_1| \neq |J_2|$. Surprisingly, this case seems to be very different as one can see already in the explicit results of [13].

Correlation functions of these type of operators consist of a very specific type of planar Feynman diagrams that have the shape of a spider web. In figure 1.b we draw an example of such a diagram for the case where $J_2 = 1$. In general, the diagrams can be constructed by first contracting all the ϕ_1 fields in the trace, (the black lines in figure 1). Then, the ϕ_2 's have no other option but to spiral around the trace, crossing the ϕ_1 lines from the right to the left, (the red line in figure 1.b). Each time a ϕ_2 line crosses a ϕ_1 line we have the four scalars interaction of the fishnet model (2.1). The absence of the complex conjugate interaction vertex forbids any other diagram to contribute in the planar limit.

2.2 Fishchain model

The holographic fishchain dual of the $\mathfrak{u}(1)$ operators of charge J_1 consists of a chain of J_1 point-like scalar particles in AdS_5 . In the classical/strong coupling limit, $\xi \rightarrow \infty$, the theory is defined by the action

$$S_{\text{dual}} = \xi \int dt \sum_{i=1}^{J_1} \left[\frac{\dot{X}_i^2}{2} + \prod_k (-X_k \cdot X_{k+1})^{-\frac{1}{J_1}} \right], \quad (2.4)$$

where $X_i \in \mathbb{R}^{1,5}$. While at the quantum level the particles live on AdS_5 space, at the classical limit its radius collapses to zero and the dynamics take place on the light cone, $X_i^2 = 0$. One can think about (2.4) as a discretized version of the gauge fixed Polyakov action for a string, which requires a Virasoro condition. An analog of the Virasoro condition in the case of the fishchain is $\dot{X}_i^2 = 1$. In addition to the constraints

$$X_i^2 = 0, \quad \dot{X}_i^2 = 1, \quad i = 1, 2, \dots, J_1 \quad (2.5)$$

the Hamiltonian of the system should vanish to ensure the time reparametrization symmetry

$$H_q = 0, \quad H_q = \text{tr} \left(\frac{q_J^2}{2} \dots \frac{q_1^2}{2} \right) - 1, \quad (2.6)$$

where q_i is the local charge density $q_i^{MN} \equiv \dot{X}_i^M X_i^N - \dot{X}_i^N X_i^M$. The classical Hamiltonian H_q follows from the action (2.4) together with the constraints (2.5), see [5].

As can be seen from figure 2, the action (2.4) produces rather non-trivial dynamics. Even though this dynamic may look chaotic, the model is integrable.

Quantization. We now briefly go through the main steps of the canonical quantization procedure. We will follow the Dirac procedure for the quantization of a system with constraints. To begin with, we notice that in addition to the primary constraints (2.5) we also have to include the secondary constraint $\dot{X}_i \cdot X_i = 0$. Using that the canonically conjugate to X_i variable is $P_i = \dot{X}_i$ we have the following constraints

$$\varphi_{i,X} = X_i^2, \quad \varphi_{i,P} = P_i^2 - 1, \quad \varphi_i = X_i \cdot P_i \quad \text{and} \quad H_q. \quad (2.7)$$

Among these, φ_j and $\varphi_{j,P}$ are second class constraints as follows from their Poisson bracket. Hence, in the quantization of the model we first introduce corresponding Dirac brackets and only then promote them into quantum commutation relations. For example, the commutator between the operators \hat{X} and \hat{P} takes a non-standard form

$$[\hat{X}_k^M, \hat{P}_j^N] = \frac{i\delta_{kj}}{\xi} \left(\eta^{MN} - \hat{P}_k^M \hat{P}_K^N \right). \quad (2.8)$$

Similarly, the commutator between different components of \hat{X}_k^M is no longer zero. To resolve these commutation relations we introduce the operator $\hat{Y}_i^N = \frac{i}{\xi} \partial_{P_{i,N}}$, which commutes in the standard way with \hat{P}_k^N . Then we show that we automatically solve all commutation relations if $\hat{X}_i^M = \hat{Y}_i^M - (\hat{Y}_i \cdot \hat{P}_i) \hat{P}_i^M$. Next, we have to impose the constraints (2.7) at the quantum level and resolve possible ordering ambiguities. What we find is that

- The quantum constraint $\hat{\varphi}_i = \hat{X}_i \cdot \hat{P}_i$ is automatically satisfied. Here, we had to choose an ordering between \hat{X}_i and \hat{P}_i in $\hat{\varphi}_i$. To satisfy the constraint, we had to correlate this choice with the one in the definition of \hat{X}_i in terms of \hat{Y}_i .
- The constraint $\hat{\varphi}_{i,X}$ is proportional to $\text{tr } q_i^2$, which is nothing but the quadratic Casimir, $\hat{\mathbf{C}}_{i,2}/\xi^2$. Instead of setting it to zero we identify it with the dimension 1 of the scalar field ϕ_1 , corresponding to $\hat{\mathbf{C}}_{i,2} = -3$.
- The constraint $\hat{\varphi}_{i,P}$ fixed the dependence of the wave function on $R_i^2 \equiv -Y_i \cdot Y_i$, as a result all the dynamical information is contained in the reduced wave-function $\Psi(Z_1, \dots, Z_J)$ depending on J coordinates Z_i^M on AdS_5 that are related to the Y_i 's via $Y_i^M = R_i Z_i^M$.
- Finally, we have to resolve the ordering ambiguity in the quantum version of H_q . Since the matrix elements of \hat{q}_i^{NM} do not commute with each other, the quantum version of q_i^2 suffers from ambiguities. As we explain below, the relevant definition is the symmetric and traceless combination

$$:\hat{q}_i^2 := \hat{q}_i^2 - \frac{2i}{\xi} \hat{q}_i - \frac{1}{\xi^2}, \quad (2.9)$$

where the charge density in the Z -coordinates is

$$\hat{q}_j^{MN} = -\frac{i}{\xi} (Z_j^N \partial_{Z_j^M} - Z_j^M \frac{\partial}{\partial Z_j^N}). \quad (2.10)$$

The corresponding quantum fishchain Hamiltonian takes the form

$$\hat{H}_q = \text{tr} \left(\frac{:\hat{q}_J^2:}{2} \dots \frac{:\hat{q}_1^2:}{2} \right) - 1. \quad (2.11)$$

At the end of the day we end with a quantum theory in AdS_5 that is defined by two relations that the fishchain wave function $\Psi(Z_1, \dots, Z_J)$ has to satisfy

$$\hat{H}_q \circ \Psi = 0, \quad \text{and} \quad \text{tr } \hat{q}_i^2 \circ \Psi = \frac{2\Delta_i(4 - \Delta_i)}{\xi^2} \Psi \quad (2.12)$$

where $\Delta_i = 1$ is the dimension of the scalar ϕ_1 .

The Holographic map. The key object which allows to establish the Holographic duality between the fishchain model and the fishnet CFT is the *CFT wave function* introduced in [5]. This is a $J + 1$ point correlator of a local operator \mathcal{O} and J scalar fields

$$\varphi_{\mathcal{O}}(x_1, \dots, x_J) = \langle \mathcal{O}(x_0) \text{tr} [\phi_1^\dagger(x_1) \dots \phi_J^\dagger(x_J)] \rangle. \quad (2.13)$$

The knowledge of this function is equivalent to specifying the local operator \mathcal{O} . In order to compute $\varphi_{\mathcal{O}}$ in perturbation theory one has to sum an infinite number of wheel diagrams like in figure 1(a). To sum these diagrams one can use the so-called graph building operator

$\hat{\mathcal{B}}$, which is an operator acting on the wave function $\varphi_{\mathcal{O}}$ by adding one more wheel to the diagrams

$$\hat{\mathcal{B}} \circ f(\vec{x}_1, \dots, \vec{x}_J) = \int \prod_{i=1}^J d^4 y_i \prod_{j=1}^J \frac{\xi^2/\pi^2}{(\vec{y}_i - \vec{y}_{i+1})^2 (\vec{y}_j - \vec{x}_j)^2} f(\vec{y}_1, \dots, \vec{y}_J) . \quad (2.14)$$

Physical non-protected operators in the CFT spectrum are in one to one correspondence with stationary wave functions

$$\hat{\mathcal{B}} \circ \varphi_{\mathcal{O}}(x_1, \dots, x_J) = \varphi_{\mathcal{O}}(x_1, \dots, x_J) . \quad (2.15)$$

The map between the CFT and the fishchain wave functions reads [5]

$$\psi_{\mathcal{O}}^{\mathbf{I}}(Z_1, \dots, Z_J) = \int \prod_{i=1}^J \frac{D^4 X_i}{-4\pi^2 (Z_i \cdot X_i)^3} \Phi_{\mathcal{O}}(X_1, \dots, X_J) , \quad (2.16)$$

where $X^{M=-1, \dots, 4}$ are six dimensional embedding coordinates with $(-, +, +, +, +, +)$ signature [14]. They realize flat four dimensional space as the protective lightcone of $\mathbb{R}^{1,5}$ as

$$X = \frac{1}{2} X^+ (1 + x^2, 1 - x^2, 2\vec{x}) . \quad (2.17)$$

In this parameterization we have for example $1/(x-y)^2 = X^+ Y^+ / (-2X \cdot Y)$. When rewriting the correlation functions in embedding space we are following the general prescription of [15]. According to it we have to introduce extra factors of X^+ in agreement with the scaling dimensions of the corresponding operators. In particular, the embedding space wave function in (2.16) is defined as

$$\Phi_{\mathcal{O}}(X_1, \dots, X_J) \equiv \frac{\varphi_{\mathcal{O}}(\vec{X}_1/X_1^+, \dots, \vec{X}_J/X_J^+)}{X_1^+ \dots X_J^+ (X_0^+)^{\Delta_{\mathcal{O}}}} . \quad (2.18)$$

The introduction of these extra factors ensures that the r.h.s. stays invariant under all conformal transformations.

It was shown in [5] that if $\phi_{\mathcal{O}}$ obeys the condition (2.15), then the l.h.s. of (2.16) will be automatically annihilated by \hat{H}_q . At the same time the second condition in (2.12) is also satisfied just because the kernel $\frac{1}{(Z \cdot X)^3}$ solves this equation for any null vector X . In the next section we will show how this Holographic map naturally generalizes to the case where both quantum numbers $J_1 = J$ and $|J_2| < J$ are non-zero.

3 CFT wave function and the graph building operator

In this section we generalize the fishchain model to include magnons i.e. insertions of the ϕ_2 fields into the “vacuum” of ϕ_1 ’s. We assume that the number of ϕ_2 fields is less the number of ϕ_1 ’s. The starting point for the construction is the *CFT wave function*, which we introduced in (2.13) for the $\mathfrak{u}(1)$ sector. Like before it is given by the $(J+1)$ -point

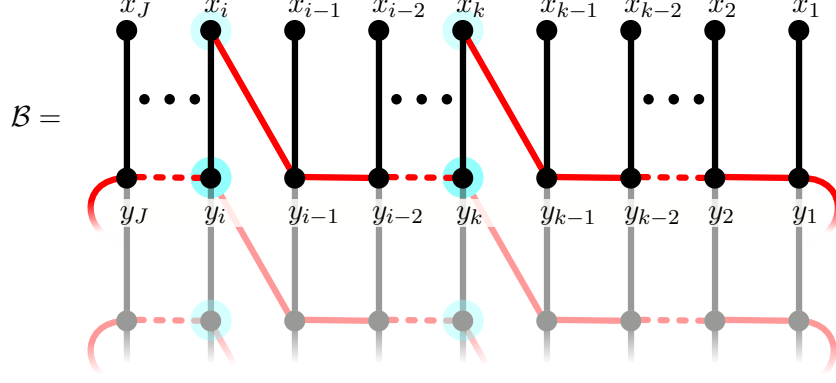


Figure 3. The graph-building operator $\hat{\mathcal{B}}$ for the state with two magnons. The locations of the magnons are indicated by the blue circles.

correlation function between a single trace operator of the type (2.3) and the trace of J local operators, see figure 1.b

$$\varphi_{\mathcal{O}}^{\mathbf{I}}(x_1, \dots, x_J) = \langle \mathcal{O}(x_0) \text{tr} [\chi_{I_1}(x_1) \dots \chi_{I_J}(x_J)] \rangle. \quad (3.1)$$

The new ingredient is that the local operators χ_a are not just single scalars ϕ_1^\dagger , but come in two types

$$\chi_0(x) = \phi_1^\dagger(x) \quad \begin{array}{c} \bullet \\ | \end{array} \quad \chi_1(x) = \phi_1^\dagger(x) \phi_2^\dagger(x) \quad \begin{array}{c} \bullet \\ | \diagdown \end{array}. \quad (3.2)$$

We use the multi-index notation $\mathbf{I} = (I_1, \dots, I_J)$ where the index $I_j \in \{0, 1\}$. For example, when $I_j = 1$ it indicates the position of the χ_1 insertion, which is a composite of two scalars ϕ_1^\dagger and ϕ_2^\dagger . Like before, the knowledge of this correlator is equivalent to the knowledge of the initial operator. Any other planar correlators, such as those with $\phi_2 \phi_2^\dagger$ and $\phi_1^\dagger \phi_1$, can be expressed in terms of this one. In section 5 we show that the order of the magnons inside the correlator can be interchanged. Hence, in order to reconstruct the local operator it is sufficient to know the CFT wave function for only one of all possible magnon orderings. In this section we consider all magnon orderings on equal footing.

As for the case with no magnons, the Feynman diagrams which contribute to the correlator $\varphi_{\mathcal{O}}^{\mathbf{I}}$ in (3.1) are of iterative structure and can be represented as a simple geometric series built from the corresponding graph building operator $1/(1 - \hat{\mathcal{B}})$. The only difference in comparison to the previous section is that now the graph building operator $\hat{\mathcal{B}}$ is slightly more complicated and is given by

$$\hat{\mathcal{B}} \circ f(x_1, \dots, x_J) \equiv \int \prod_{i=1}^J d^4 y_i \left(\prod_{j=1}^J b_{I_j}(x_j, y_j, y_{j-1}) \right) f(\vec{y}_1, \dots, \vec{y}_J), \quad (3.3)$$

where f is a probe function. In (3) the integration kernel is built out of elementary building

blocks b_a , which are different for the sites with magnons and without

$$b_I(x, y, \tilde{y}) = \frac{\xi^2}{\pi^2(x-y)^2} \times \begin{cases} \frac{1}{(y-\tilde{y})^2} & I = 0 \text{ (no magnon)} \\ \frac{1}{(x-\tilde{y})^2} & I = 1 \text{ (magnon)} \end{cases}. \quad (3.4)$$

We see that at the sites with a magnon, the ϕ_2 propagator connects to the external point x_j instead of the integrated y_j point as in a site without a magnon. This is illustrated in figure 3, where the sites with magnons are highlighted by the blue circles.

As we explained in the previous section the key equation which the CFT wave function should satisfy is (2.15). The wave function is the correlator computed at some finite value of the coupling ξ . It is given by an infinite sum of planar Feynman diagrams. As such it should stay invariant under addition of an extra layer i.e. the wave function should be an eigenstate of the graph building operator with a unit eigenvalue, (2.15). For explicit examples we refer to [13]. As was demonstrated in [13] the condition (2.15) singles out the physical states in the theory and leads to the discrete spectrum of the scaling dimensions Δ corresponding to the properly regularized and renormalized single trace operators of the type (2.3). Like in our previous paper [5], we will now rewrite (2.15) in a form suitable for uplifting to AdS_5 space and show that the dynamics induced by (2.15) is exactly this of the quantum fishchain (QFC).

3.1 Inverting the graph building operator

Following [5] in order to relate the graph building operator \mathcal{B} to the dual fishchain model in AdS_5 , we have to invert it and rewrite (2.15) as a zero energy Hamiltonian constraint

$$\hat{H} |\varphi_{\mathcal{O}}\rangle \equiv \left(\hat{\mathcal{B}}^{-1} - 1 \right) |\varphi_{\mathcal{O}}\rangle = 0. \quad (3.5)$$

This constraint is then interpreted as the result of a time reparametrization symmetry of the fishchain. We show below that, defined in this way, $\hat{\mathcal{B}}^{-1}$ and \hat{H} are differential operators.

In the case without magnons the inversion of $\hat{\mathcal{B}}$, given by (2.14), was straightforward. We simply act with \square_j on all the external x_k points in (2.14). This has the effect of eliminating the corresponding y_k integrals and the $1/(4\pi^2(x_i - y_i)^2)$ factors.⁴ In the case at hand we have an extra complication – there are two propagators that end at a site with a magnon. Acting with \square_j on the magnon site does not remove the integration anymore, see figure 3.

Let us show that the inversion of \mathcal{B} is still possible in the situation when there is at least one site without a magnon, i.e. for $J_2 < J_1$. Without loss of generality, we assume that there is a magnon on the k 'th site, but there is no magnon at the neighboring site to the right i.e. $I_{k-1} = 0$, $I_k = 1$, see figure 4. In this case we can hit x_{k-1} with \square_{k-1} , removing the integration in y_{k-1} . After that the propagator connecting y_{k-1} (which is now equal to x_k) with x_k can be removed by multiplication with $x_{k,k-1}^2$.⁵ After this we are left

⁴Recall that $\square_i \frac{1}{4\pi^2(x_i - y_i)^2} = -\delta^4(x_i - y_i)$.

⁵We use the standard notation $x_{ab} = x_a - x_b$.

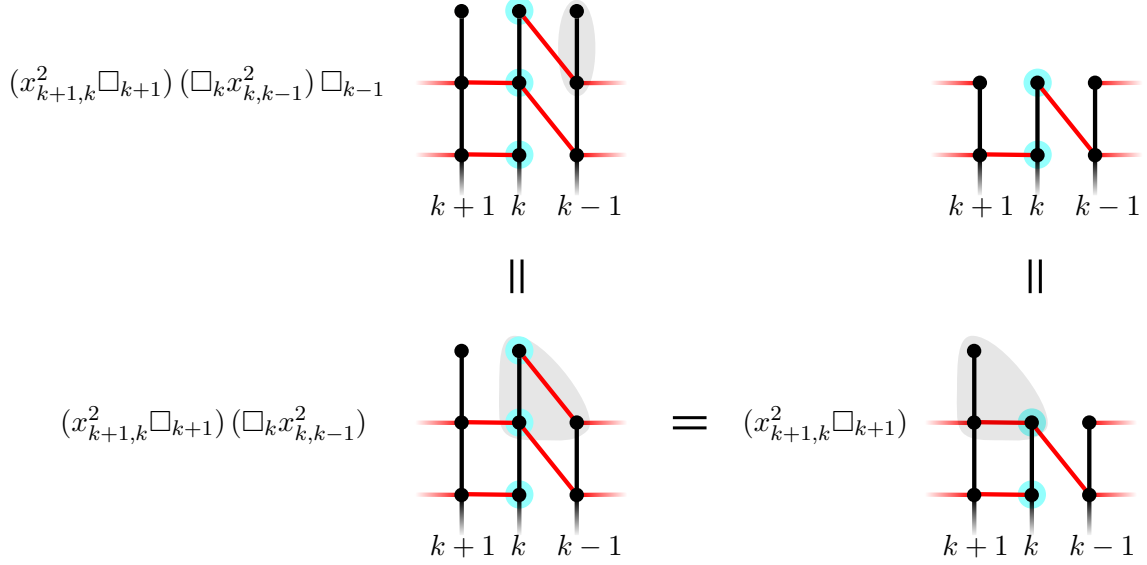


Figure 4. In the presence of a magnons, the inverse of the graph building operator is more involved. Here, we demonstrate how the operator is inverted for the case where there is a magnon at the k 'th site but no magnons at the neighboring sites.

with a single propagator connecting x_k with an integration point y_k , which now can be treated with \square_k .

It is easy now to figure out the general procedure. Assuming again that at the site $k-1$ there is no magnon we begin by acting with \square_{k-1} , removing integration in y_k . Then, if at the site k there is a magnon, we act with the combination $\square_k x_{k,k-1}^2$, see figure 4. Otherwise, on the sites with no magnon we act with the operator $x_{k,k-1}^2 \square_k$. Acting in this way we can invert $\hat{\mathcal{B}}$ completely. For example for $J=3, M=1$ with $I_3=0, I_2=1$ and $I_1=0$ we find

$$\hat{\mathcal{B}}^{-1} = \frac{1}{(-4\xi^2)^3} x_{1,3}^2 (x_{2,3}^2 \square_3) (\square_2 x_{2,1}^2) \square_1. \quad (3.6)$$

We conclude that it is always possible to write $\hat{\mathcal{B}}^{-1}$ as a differential operator. Below we rewrite $\hat{\mathcal{B}}^{-1}$ in a simple and manifestly conformally invariant way, applicable for all cases. For that we will have to first change to embedding coordinates, introduced in section 2.2.

Embedding coordinates. When manipulating conformal integrals such as the ones that are generated by the graph building operator, it is always advantageous to work in the embedding coordinates. In the case of the correlator (3.1), we have the χ_I operators in (3.2) at positions X_1, \dots, X_J and \mathcal{O}_Δ at X_0 . Hence, the corresponding embedding space wave function is defined as

$$\Phi_{\mathcal{O}}^{\mathbf{I}}(X_1, \dots, X_J) \equiv \frac{\varphi_{\mathcal{O}}^{\mathbf{I}}(\vec{X}_1/X_1^+, \dots, \vec{X}_J/X_J^+)}{(X_1^+)^{1+I_1} \dots (X_J^+)^{1+I_J} (X_0^+)^{\Delta_{\mathcal{O}}}}. \quad (3.7)$$

The advantage of the covariant formalism is that the inverted $\hat{\mathcal{B}}$ can be written in a very concise form

$$\hat{\mathcal{B}}^{-1} = \text{tr} (\beta_{J,I_J} \dots \beta_{1,I_1}) \quad (3.8)$$

where β_{k,I_k} is a local operator that only acts on the X_k 'th coordinate. It is given by

$$(\beta_{k,I_k})^{MN} = -\frac{1}{2} \times \begin{cases} X_k^M X_k^N K_k^2 & I_k = 0 \\ X_k^M K_k^2 X_k^N & I_k = 1 \end{cases}, \quad \text{where} \quad K^M = -\frac{i}{\xi} \frac{\partial}{\partial X_M}. \quad (3.9)$$

To understand the mechanism behind (3.8) we look at the same example as in (3.6). There we took $I_3 = 0$, $I_2 = 1$ and $I_1 = 0$. For this case (3.8) gives

$$\mathcal{B}^{-1} = \frac{1}{(-2)^3} (X_3 \cdot X_1) (X_3 \cdot X_2) K_3^2 K_2^2 (X_2 \cdot X_1) K_1^2. \quad (3.10)$$

By noticing that $-\xi^2 K_i^2 = \square_i^{4D} - 4\partial_{X_i^+} \partial_{X_i^-}$ and due to the fact that $\Phi_{\mathcal{O}}^{\mathbf{I}}$ from (3.7) does not depend on X_- , we can simply replace K_i^2 by $-\frac{1}{\xi^2} \square_i$ when acting on the CFT wave function. In addition we use $x_{ab}^2 = \frac{-2X_a \cdot X_b}{X_a^+ X_b^+}$ to reproduce precisely (3.6). It is equally easy to see that the equation (3.8) works in the general situation, provided that $J_2 < J_1$.

Finally, let us rewrite the local site operators, β_{k,I_k} , in terms of the local generator of the conformal symmetry, namely in terms of \mathfrak{q}_k defined as

$$\hat{\mathfrak{q}}_i^{MN} \equiv X_i^N K_i^M - X_i^M K_i^N. \quad (3.11)$$

We can use that the CFT wave function is a homogeneous function of X_k with degree of homogeneity $-(1 + I_k)$, as follows directly from its definition (3.7). This property allows us to make the replacements $\hat{X}_k \cdot \hat{K}_k \rightarrow \frac{i}{\xi} (1 + I_k)$. Using that in analogy with (2.9), we find

$$\beta_{j,I_j}^{MN} \simeq (\hat{\mathfrak{q}}_k^2)^{MN} - \frac{i}{\xi} (2 + I_k) \mathfrak{q}_k^{MN} - \frac{1}{\xi^2} (1 + I_k) \eta^{MN}. \quad (3.12)$$

where the " \simeq " means equality when acting on the wave function (3.7).

The strong coupling classical limit. Before we proceed to the holographic interpretation of equation (3.8) at the quantum level, we can already make a nontrivial conclusion about the strong coupling limit of the theory, where the dual description becomes classical [4].

In order to understand the classical limit we recall that the operator $(\mathcal{B}^{-1} - 1)$ can be interpreted as a worldline Hamiltonian. The classical limit is obtained by simply replacing $-\frac{i}{\xi} \partial_{x_i}$ by the classical momentum p_i [4]. As one can see from e.g. (3.9) the only difference between the situation with magnon and without magnon is the ordering of the operators X_i and K_i , which becomes irrelevant in the classical limit. From this simple observation we conclude that the classical theory is not affected by the presence of magnons. But there will be a difference visible already at the first quasi-classical correction.

One way to think about this is that in the strong coupling limit the difference between a dimension one scalar and a dimension two composite operator made of two scalars (which is the magnon), becomes negligible. Namely, in units of $1/\xi$, both of them are indistinguishable from zero.

3.2 Quantum fishchain with magnons

In the previous section we understood that the classical limit of the theory with or without magnons should be the same. This means that essentially all the quantization procedure developed in [5] and described shortly in section 2.2 still applies here. There are only two steps in our quantization procedure which allow for a modification. First, in (2.12) we assumed that the local Casimir operator $\text{tr } \hat{q}_i^2$, which is a c-number, should be associated with the dimension of the scalar, or more precisely its AdS_5 mass $m^2 = -3$. This assumption does not look natural anymore as the magnons are the bound-states of two scalars ϕ_1^\dagger and ϕ_2^\dagger of the total dimension $\Delta_i = 2$, meaning that the AdS_5 mass becomes -4 or equivalently $\text{tr } \hat{q}_i^2 = \frac{8}{\xi^2}$.

Another subtle point in the quantization procedure, which needs to be revisited, is the ordering ambiguity in the quantum Hamiltonian \hat{H}_q (see (2.11) and (2.9)). We have a freedom to add to the naive term $(\hat{q}_i^2)^{NM}$ the extra terms $(\hat{q}_i)^{NM}$ and $\eta^{NM} \text{tr } q_i^2 \sim \eta^{NM}/\xi^2$ like in (2.9). The general ansatz is

$$(q_k^2)^{NM} \rightarrow: (q_k^2)^{NM} :_{I_k} = (\hat{q}_k^2)^{NM} - i \frac{c_{I_k}}{\xi} \hat{q}_k^{NM} - \frac{d_{I_k}}{\xi^2} \eta^{NM}, \quad (3.13)$$

where c_{I_k} and d_{I_k} are some numbers, which for the case with no magnons were set to 2 and 1 correspondingly i.e. $c_0 = 2$, $d_0 = 1$. In this section we fix this quantization ambiguity by requiring that this quantum fishchain model is exactly dual to the Fishnet model for the states with magnons.

Map between the wave functions. In [5] we have built an explicit map between the CFT wave function in the $\mathfrak{u}(1)$ -sector and the wave function of the quantum fishchain in AdS_5 . This construction was reviewed in section 2.2, see (2.16). We now extend this map to the case with magnons.

The map (2.16) takes the 4D flat space CFT wave function and returns a function of J points Z_1, \dots, Z_J , parametrizing a unit radius AdS_5 space, $Z_i^2 = -1$. These are the coordinates of the particles constituting the fishchain.

The factors $1/(Z_i \cdot X_i)^3$ in (2.16) are bulk to boundary propagators for J scalars in AdS_5 of mass $m^2 = -3$. It was designed to solve the constraint $\text{tr } \hat{q}_i^2 = \frac{6}{\xi^2}$. As for the sites with magnons we should modify this constraint to $\text{tr } \hat{q}_i^2 = \frac{8}{\xi^2}$, so we can take $1/(Z_i \cdot X_i)^2$. Hence, the generalization of the map (2.16) to wavefunctions with both χ_0 and χ_1 operators is

$$\psi_{\mathcal{O}}^{\mathbf{I}}(Z_1, \dots, Z_J) = \int \prod_{i=1}^J \frac{D^4 X_i}{-4\pi^2 (Z_i \cdot X_i)^{3-I_i}} \Phi_{\mathcal{O}}^{\mathbf{I}}(X_1, \dots, X_J). \quad (3.14)$$

As before, $1/(Z_i \cdot X_i)^2$ is the bulk to boundary propagator for an AdS_5 scalar of $m^2 = -4$. It is the fastest decaying solution to the bulk equation of motion with a source at the boundary point X_i .⁶

It is not too hard to invert the map (3.14). One way is to go to the boundary of AdS_5 . While with no magnon excitations the bulk wave function exactly reduces to the CFT wave

⁶The other solution is $\log(Z_i \cdot X_i)/(Z_i \cdot X_i)^2$.

function [5], in the case with magnons there is an addition logarithmic factor

$$\lim_{Z_i^+ \rightarrow \infty} \frac{\psi_{\mathcal{O}}^{\mathbf{I}}(Z_1, \dots, Z_J)}{\prod_i (2 \log Z_i^+)^{I_i}} = \Phi_{\mathcal{O}}^{\mathbf{I}}(Z_1, \dots, Z_J) . \quad (3.15)$$

Exact duality. Having the map between the wave functions extended to the general case (3.14), we can prove the duality and also fix the remaining quantization ambiguity manifested by the existence of two arbitrary constants in the QFC Hamiltonian (3.13). Following [5] we can establish the map between the QFC Hamiltonian \hat{H}_q and the CFT Hamiltonian H by requiring

$$\hat{H}_q \circ \psi_{\mathcal{O}}^{\mathbf{I}}(Z_1, \dots, Z_J) = \int \prod_{i=1}^J \frac{D^4 X_i}{-4\pi^2 (Z_i \cdot X_i)^{3-I_i}} H \circ \Phi_{\mathcal{O}}^{\mathbf{I}}(X_1, \dots, X_J) = 0 , \quad (3.16)$$

where $H = (\hat{\mathcal{B}}^{-1} - 1)$ as defined in (3.5). Exactly like in [5] we simply use the identity

$$\int \prod_{i=1}^J \frac{D^4 X_i}{-4\pi^2 (Z_i \cdot X_i)^{3-I_i}} \hat{q}_i F(X_1, \dots, X_J) = \hat{q}_i \int \prod_{i=1}^J \frac{D^4 X_i}{-4\pi^2 (Z_i \cdot X_i)^{3-I_i}} F(X_1, \dots, X_J) , \quad (3.17)$$

where the q 's are the $SO(1,5)$ isometry generators of AdS_5 , (2.10). From this we immediately establish the values of the missing constants in (3.13) by reading them off (3.12): $c_{I_k} = 2 + I_k$ and $d_{I_k} = 1 + I_k$. Thus we arrive at the fishchain quantum Hamiltonian constraint

$$\hat{H}_q = \text{tr} \left[\frac{\hat{q}_J : I_J}{2} \dots \frac{\hat{q}_1 : I_1}{2} \right] - 1 . \quad (3.18)$$

Here, $: q_k :_{I_k}$ is given by

$$(: q_k^2 :_{I_k})^{MN} \equiv (q_k^2)^{MN} - \frac{i}{\xi} (2 + I_k) q_k^{MN} - \frac{1}{\xi^2} (1 + I_k) \eta^{MN} . \quad (3.19)$$

This derivation extends the proof [5] of the exact duality between the QFC and the Fishnet CFT models beyond the $\mathfrak{u}(1)$ sector.

Note that so far we only considered the CFT wave functions, which contained ϕ_1^\dagger and $\phi_1^\dagger \phi_2^\dagger$ under the correlator with a local operator \mathcal{O} . Whereas this does indeed go beyond the $\mathfrak{u}(1)$ sector one could still question if that is the most general case. In particular one can also introduce “anti-magnons” i.e. $\phi_2 \phi_1^\dagger$, as we do in the next subsection. Later, however, we show that the CFT wave functions with the same magnon number J_2 (defined as a difference of the number of magnons and anti-magnons) are all equivalent to each other. It is yet very fruitful to have both magnons and anti-magnons at the same time as we will see in the next section 3.3.

3.3 Adding anti-magnons to the QFC

We consider the most general situation, where at a site of the chain we can have either no magnon, one magnon, one anti-magnon or a magnon–anti-magnon pair. The CFT wave

function definition (3.1) should be extended by allowing for χ_j to take two additional values

$$\chi_{-1}(x) = \phi_2(x)\phi_1^\dagger(x) \quad \chi_{\bar{0}}(x) = \phi_2(x)\phi_1^\dagger(x)\phi_2^\dagger(x) \quad (3.20)$$

for anti-magnon and magnon–anti-magnon pair correspondingly. All the steps from the previous parts of this section are carried out in a similar way. We summarize in table 1 the key elements.

type	I_k	χ_{I_k}	$-2\beta_{I_k}^{MN}$	c_{I_k}	d_{I_k}	Δ_k	$\text{tr } q_k^2$
no magnon	0	ϕ_1^\dagger	$X^M X^N K^2$	2	1	1	$6/\xi^2$
magnon	+1	$\phi_1^\dagger \phi_2^\dagger$	$X^M K^2 X^N$	3	2	2	$8/\xi^2$
anti-magnon	-1	$\phi_2 \phi_1^\dagger$	$X^N K^2 X^M$	1	0	2	$8/\xi^2$
magnon + anti-magnon	$\bar{0}$	$\phi_2 \phi_1^\dagger \phi_2^\dagger$	$K^2 X^M X^N$	2	1	3	$6/\xi^2$

Table 1. Four types of local composite operators entering into the definition of the CFT wave function.

As before we assume that $|M - \bar{M}| < J$ where M is the total number of magnons and \bar{M} is the total number of anti-magnons. In this case we again have $\hat{\mathcal{B}}^{-1} = \text{tr } (\beta_{J, I_J} \dots \beta_{1, I_1})$ where the β 's are summarized in table 1.

Next, one can also map the CFT wave function with the QFC wave function in AdS_5 using the generalization of (3.14)

$$\Psi^{\mathbf{I}}(Z_1, \dots, Z_J) = \int \prod \frac{D^4 X_i}{-4\pi^2} \frac{\Phi^{\mathbf{I}}(X_1, \dots, X_J)}{(X_1.Z_1)^{4-\Delta_1} \dots (X_J.Z_J)^{4-\Delta_J}} \quad (3.21)$$

where again Δ_k is the conformal dimensions of χ_{I_k} , given in the table 1. Finally, the QFC Hamiltonian \hat{H}_q is obtained by uplifting the CFT Hamiltonian \hat{H} , which results in fixing the quantization ambiguity parameters c_I and d_I as shown in the table 1.

To summarize, we see that the quantum fishchain naturally generalizes to incorporate magnons. They are in one to one correspondence with all possible orderings of K_k^2 and the X_k 's in the site operator β_k .

4 Integrability of the fishchain with magnons

In this section we extend the proof of the quantum integrability of the QFC [5] to the general case with magnons. In order to demonstrate the integrability of the QFC model we will follow the same steps as in [5]. The strategy is to identify the Hamiltonian as a part of a large family of mutually commuting operators, which can be obtained as an expansion in powers of u of the T-operators $\hat{\mathbb{T}}(u)$.

There are 3 non-trivial T-operators, which should contain a complete set of integrals of motion. The building blocks for these operators are the Lax matrices in antisymmetric finite-dimensional representations of $\mathfrak{sl}(4)$. They were computed in [5] in terms of \hat{q}_k . We

will see that this derivation is general enough to accommodate the current case as well. The main building blocks for the operators $\hat{\mathbb{T}}(u)$ are the L-matrices

$$\begin{aligned}
\hat{\mathbb{L}}_k^{\mathbf{1}}(u) &= 1 \\
\hat{\mathbb{L}}_k^{\mathbf{4}}(u) &= u - \frac{i}{2} \hat{q}_k^{MN} \Sigma_{MN} \\
\hat{\mathbb{L}}_k^{\mathbf{6}}(u) &= u^2 + u \hat{q}_k + \frac{\hat{q}_k^2}{2} - \frac{i \hat{q}_k}{\xi} - \frac{\text{tr } \hat{q}_k^2}{8} + \frac{1}{4\xi^2} \\
\hat{\mathbb{L}}_k^{\mathbf{4}}(u) &= \left(u^2 - \frac{1}{8} \text{tr } \hat{q}_k^2 + \frac{1}{\xi^2} \right) \left[-\hat{\mathbb{L}}_k^{\mathbf{4}}(-u) \right]^T \\
\hat{\mathbb{L}}_k^{\mathbf{1}}(u) &= \left(u^2 - \frac{1}{8} \text{tr } \hat{q}_k^2 + \frac{5}{4\xi^2} \right)^2 + \frac{1}{8\xi^2} \text{tr } \hat{q}_k^2 - \frac{1}{\xi^4}.
\end{aligned} \tag{4.1}$$

Where Σ_{MN} are 6-dimensional σ -matrices. Their explicit representation can be found in [5]. The mutually commuting families of operators are constructed from (4.1) via

$$\hat{\mathbb{T}}(u) = \text{tr} \left[\hat{\mathbb{L}}_J(u - \theta_J) \dots \hat{\mathbb{L}}_2(u - \theta_2) \hat{\mathbb{L}}_1(u - \theta_1) G \right]. \tag{4.2}$$

Where G is a constant *twist* matrix and $\{\theta_j\}$ are the so-called inhomogeneities which can be taken as arbitrary. For the original fishnet model the twist matrix is trivial, $G = 1$. However, here we consider the most general deformed case, dual to the twisted fishnet of [16], with $G = \text{diag}(\lambda_1, \lambda_2, \lambda_3, \lambda_4)$ and we assume $\lambda_1 \lambda_2 \lambda_3 \lambda_4 = 1$ for unimodularity of G . Next, we have to choose the values of $\{\theta_j\}$ so that the QFC Hamiltonian appears in (4.2) for a special value of u . More precisely we require that in the same manner as in the case without magnons we have $\hat{\mathbb{T}}^{\mathbf{6}}(0) = \hat{H}_q + 1$.

We now consider all 4 cases of insertions one by one – the site without magnon, with magnon, with anti-magnon, and with magnon anti-magnon pair using the data from table 1.

No-magnon case. The case without magnon corresponds to a single scalar ϕ_1 , which allows for the value of the quadratic Casimir to be -3 , implying $\text{tr } \hat{q}_k^2 = \frac{6}{\xi^2}$. As a result (4.1) reduces to

$$\begin{aligned}
\hat{\mathbb{L}}_k^{\mathbf{6}}(u) &= u^2 + u \hat{q}_k + \frac{\hat{q}_k^2}{2} - \frac{i \hat{q}_k}{\xi} - \frac{1}{2\xi^2} \\
\hat{\mathbb{L}}_k^{\mathbf{4}}(u) &= \left(u^2 + \frac{1}{4\xi^2} \right) \left[-\hat{\mathbb{L}}_k^{\mathbf{4}}(-u) \right]^T \\
\hat{\mathbb{L}}_k^{\mathbf{1}}(u) &= u^2 \left(u^2 + \frac{1}{\xi^2} \right),
\end{aligned} \tag{4.3}$$

we see that $\hat{\mathbb{L}}_k^{\mathbf{6}}(0) = \frac{\hat{q}_k^2}{2} - \frac{i \hat{q}_k}{\xi} - \frac{1}{2\xi^2} = \frac{:\hat{q}_k^2:0}{2}$, which is the correct factor in \hat{H}_q for sites without a magnon, meaning that for these sites we have to set $\theta_k = 0$.

Magnon case. For the site with magnon the dimension $\Delta_k = 2$ corresponds to the quadratic Casimir -4 , implying that $\text{tr } \hat{q}_k^2 = \frac{8}{\xi^2}$. Consequently from (4.1) we get

$$\begin{aligned}\hat{\mathbb{L}}_k^{\mathbf{6}}(u) &= u^2 + u\hat{q}_k + \frac{\hat{q}_k^2}{2} - \frac{i\hat{q}_k}{\xi} - \frac{3}{4\xi^2} \\ \hat{\mathbb{L}}_k^{\mathbf{4}}(u) &= u^2 \left[-\hat{\mathbb{L}}_k^{\mathbf{4}}(-u) \right]^T \\ \hat{\mathbb{L}}_k^{\mathbf{1}}(u) &= \left(u + \frac{i}{2\xi} \right)^2 \left(u - \frac{i}{2\xi} \right)^2.\end{aligned}\tag{4.4}$$

This time the ambiguity constants are $c_I = 3$ and $d_I = 2$ i.e. we need to tune θ_k to obtain $\hat{\mathbb{L}}_k^{\mathbf{6}}(-\theta_k) = \frac{\hat{q}_k^2}{2} - \frac{3i\hat{q}_k}{2\xi} - \frac{1}{\xi^2}$. Note that with only one parameter θ_k it is not guaranteed that we manage to fit the two constants correctly. Fortunately, by setting $\theta_k = \frac{i}{2\xi}$ ⁷ we indeed obtain $\hat{\mathbb{L}}_k^{\mathbf{6}}(0) = \frac{1}{2} : \hat{q}_k^2 :_1$.

Anti-magnon case. The building block for the anti-magnon is $\hat{\mathbb{L}}_k^{\mathbf{6}}(-\theta_k) = \frac{\hat{q}_k^2}{2} - \frac{i\hat{q}_k}{2\xi} - \frac{1}{\xi^2}$, which corresponds to $\theta_k = -\frac{i}{2\xi}$.

Magnon-anti-magnon case. The Lax matrix, in this case, is identical to the no-magnon case considered above. The reason is that $\Delta(\chi_{\bar{0}}) = 4 - \Delta(\chi_0) = 3$, so the quadratic Casimir, given by $c = \Delta(\Delta - 4) = -3$ is exactly the same as that for $\Delta = 1$. This implies that in both cases we have $\text{tr } \hat{q}_k^2 = \frac{6}{\xi^2}$. Moreover, the quantization ambiguity constants c_I and d_I are also exactly the same (see table 1) and therefore $\theta_k = 0$ in this case as well. As is explained in the next section, at the fishnet side both the magnon-anti-magnon case and no-magnon case describe different ways of cutting the same propagation line of ϕ_1 along the fishnet diagrams. Hence, the corresponding transfer matrix that encodes all physical charges should be the same.

To summarize, we see that after fixing the impurities to $\theta_k = \frac{iI_k}{2\xi}$ we get indeed $\hat{\mathbb{T}}^{\mathbf{6}}(0) = \hat{H}_q + 1$. This property implies the quantum integrability of our model, as we identified the Hamiltonian of the system within a large family of mutually commuting operators.⁸

In the current formulation the ordering of the magnons is quite important. Different distributions of magnons within the chain will produce different Hamiltonian and T-operators. We will see in section 6 that the eigenvalues of all T-operators are in fact independent of the order of magnons. This invariance has a very nice physical interpretation – it can be associated with the discrete reparametrization symmetry of the fishchain as we discuss in the next section 5. Based on the results of this section, in section 6 we present the general integrability formalism for the spectrum of the theory.

⁷N.G. is grateful to V.Kazakov and Z.Tsuboi for discussing the possibility of inclusion of inhomogeneities in relation to the magnons.

⁸Of course one should verify that there are sufficiently many independent integrals of motion. This is usually rather hard to verify rigorously, but we strongly believe this is the case. The rough counting of the integrals of motions indeed gives $\sim 4J$, which coincides with the number of degrees of freedom of the theory.

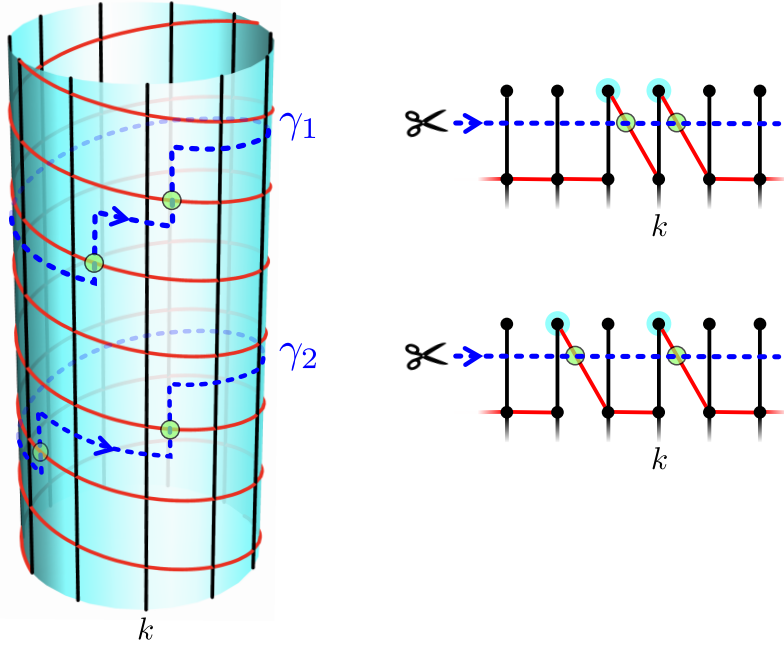


Figure 5. Two possible cuttings of the two point function of two local operators \mathcal{O} . Each cutting represents the same two point function as a contraction of two CFT wave functions. The two cuts produce different ordering of the magnons inside the chain. The cut γ_1 leads to the wave function (3.1) with $\{I_{k+3}, I_{k+2}, I_{k+1}, I_k, I_{k-1}, I_{k-2}\} = \{0, 0, 1, 1, 0, 0\}$, while the cut γ_2 leads to the equivalent wave function with $\{I_{k+3}, I_{k+2}, I_{k+1}, I_k, I_{k-1}, I_{k-2}\} = \{0, 1, 0, 1, 0, 0\}$.

5 Discrete reparametrization symmetry

When introducing the magnons we have to face the following paradox. On the CFT side, the primary operators with several magnons will be given by a complicated linear combination of all possible magnon permutations. At the same time on the fishnet side, it looks like we have the freedom to choose any ordering for the magnons. This choice is made explicitly in our definition of the CFT wave function by the correlator (2.3). Moreover, the fishchain Hamiltonian \hat{H}_q itself depends on a particular fixed order. The danger is that the spectrum of the Hamiltonian is also order dependent, which would result in an inconsistency of our approach. The physical quantities such as dimensions of local operators should not depend on an arbitrary choice of order of insertions of ϕ_2 fields in the CFT wave function, which probes this local operator.

In this section we demonstrate that, luckily, the spectrum does not depend on the ordering of the magnons. This is due to a novel symmetry of the fishchain which we interpret as the *discrete reparametrization* symmetry. We will show that redistribution of the magnons can be understood as a map between Hilbert spaces of the two chains, which differ by the magnon positions. We will then prove that this map preserves the eigenvalues of \hat{H}_q and of all other conserved charges encoded into $\hat{\mathbb{T}}(u)$, introduced in the previous section.

5.1 Cutting and leveling

Consider a correlation function between two local operators of the type (2.3) that consists of $J_1 = J$ fields ϕ_1 and $J_2 = M$ insertions of ϕ_2 's fields in the trace (as before we assume $M < J$). The planar Feynman diagrams that contribute to this correlator have cylindrical topology and are of an iterative spider-net-like structure as discussed in the introduction, see figure 5. The fishchain state, as given by the correlator in (3.1), corresponds to a specific choice of cut around this cylinder. For example the blue cut γ_1 in figure 5 corresponds to the correlator (3.1) with $M = 2$, where one magnon (χ_1) is at the k 'th site of the chain and the second magnon is at the neighboring $k + 1$ site. On the other hand, when the same diagram is cut as is indicated by the γ_2 cut in figure 5, the second magnon is at the $k + 2$ site.

In general, a cut is a choice of a decomposition of the fishnet diagrams. It is specified by a line γ that goes around the cylinder and crosses a set of propagators on the way. Here, we choose to restrict our consideration to *space-like cuts*. These are cuts that cross every ϕ_1 line and every ϕ_2 line exactly once. Moreover, every ϕ_2 cut must be followed by a ϕ_1 cut. These are the cuts that look space-like on the fishnet lattice. They are the ones that allow us to obtain all the higher loop fishnet diagrams by iterative action of the corresponding graph building operator. Such cuts are analogues to Cauchy surfaces on the string worldsheet. The graph building operator generates the “worldsheet” time propagation on such surfaces.

We notice that a choice of space-like cut corresponds to a choice of a basis of CFT wave functions of the type (2.3) as follows. A cut of a ϕ_1 -propagator is mapped to a ϕ_1^\dagger field in the corresponding correlator (2.3) and a cut of a ϕ_2 -propagator is mapped to a ϕ_2^\dagger field (see figure 5). We then merge ϕ_1^\dagger and ϕ_2^\dagger fields to be at the same point as a χ_1 or χ_{-1} in accordance with the vertex above the cut. We will give more explicit examples below.

Let us point out that the situation in which two different cuts result in a different order of magnons in the chain like in figure 5 is not the most general. In fact one can also generate an arbitrary number of magnon–anti-magnon pairs. For example, we can start with a chain with no magnons at all and deform the cut. After doing so, we end up with a magnon and an anti-magnon, see figure 6.

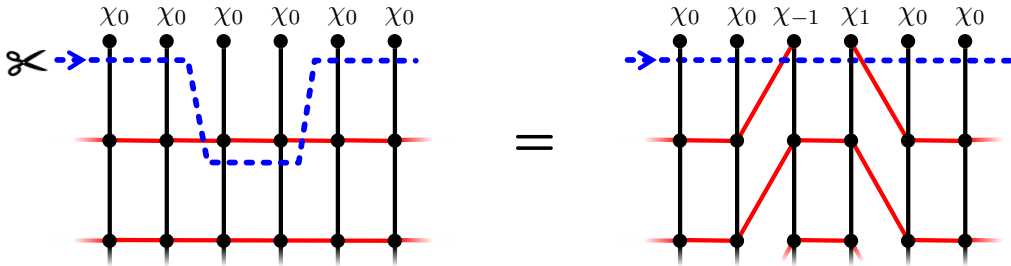


Figure 6. Another example of a cut which, instead of moving magnons around, creates a magnon–anti-magnon pair.

One way to think about the difference between different cuts is as a map between Hilbert spaces. We will now construct explicit operators that implement this map between

the Hilbert spaces of two different deformations of the cut.

5.2 The cut deformation operators

Any deformation of the cut, such as the one in figure 4, can be realized as the action of a *cut deformation operator* on the corresponding CFT wave function. The aim of this section is to construct the CFT cut deformation operators and then lift them into an operator acting on fishchain wavefunctions, i.e. acting on the AdS_5 variables Z_i . We will use these operators in section 6 and will prove that they generate a discrete symmetry of the quantum fishchain, leaving the spectrum invariant.

Any cut deformation of the CFT wave function can be decomposed into a combination of two elementary operations

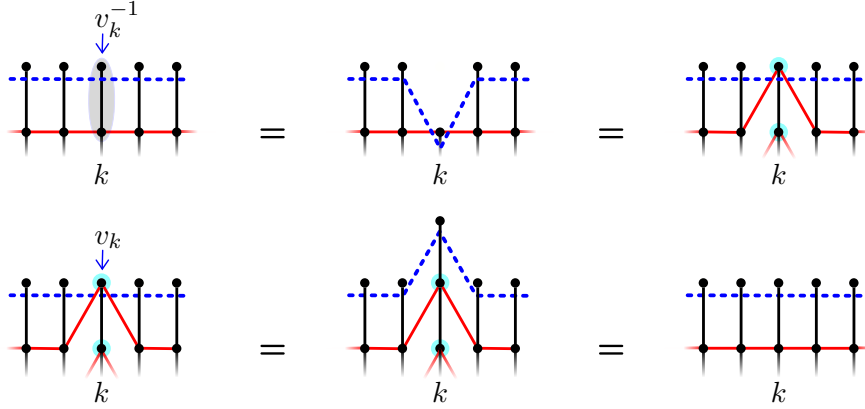


Figure 7. Graphical representation of the action of the operators v_k^{-1} and v_k on a CFT wave function. The operator v_k^{-1} removes a vertical ϕ_1 propagator, which is equivalent to the creation of a magnon–anti-magnon pair on one site. Correspondingly, v_k annihilates the magnon–anti-magnon pair.

$$v_k \circ \Psi(\dots, X_k, \dots) = \frac{\xi^2}{\pi^2} \int D^4 Y_k \frac{\Psi(\dots, Y_k, \dots)}{-2X_k \cdot Y_k} \quad (\text{add vertical propagator}) \quad (5.1)$$

$$h_{k+1,k} \circ \Psi(\dots, X_{k+1}, X_k, \dots) = \frac{\Psi(\dots, X_{k+1}, X_k, \dots)}{-2X_{k+1} \cdot X_k} \quad (\text{add horizontal propagator}) \quad (5.2)$$

As one can see from the equation the v_k operator adds a vertical ϕ_1 propagator, and h_k adds a horizontal ϕ_2 propagator. The corresponding inverse of these elementary operations are

$$v_k^{-1} = -\frac{1}{4\xi^2} \square_k \quad (\text{remove vertical propagator}) \quad (5.3)$$

$$h_{k+1,k}^{-1} = -2X_{k+1} \cdot X_k \quad (\text{remove horizontal propagator}) \quad (5.4)$$

We can build out of v and h the operators which move a magnon/anti-magnon to the right/left

$$r_{k+1,k} \equiv h_{k+1,k}^{-1} \circ v_k^{-1} \quad (\text{moves magnon right}) \quad (5.5)$$

$$\bar{r}_{k+1,k} \equiv h_{k+1,k}^{-1} \circ v_{k+1}^{-1} \quad (\text{moves anti-magnon left}) \quad (5.6)$$

Let us show that the operators v_k , $r_{k+1,k}$, $\bar{r}_{k+1,k}$ and $h_{k+1,k}^{-1}$ constitute the 3 elementary moves which allow us to map any CFT wave function to a standard form. When acting on a state in a fishchain Hilbert space, characterized by the indexes \mathbf{I} , they transform it to a state in a different Hilbert space, characterized by a different set of indexes $\tilde{\mathbf{I}}$ as follows

$$v_k : \mathbf{I} = \{\dots I_{k+1}, \bar{0}, I_{k-1} \dots\} \rightarrow \tilde{\mathbf{I}} = \{\dots I_{k+1}, 0, I_{k-1} \dots\} \quad (5.7)$$

$$r_{k+1,k} : \mathbf{I} = \{\dots I_{k+2}, 1, 0, I_{k-1} \dots\} \rightarrow \tilde{\mathbf{I}} = \{\dots I_{k+2}, 0, 1, I_{k-1} \dots\} \quad (5.8)$$

$$\bar{r}_{k+1,k} : \mathbf{I} = \{\dots I_{k+2}, 0, -1, I_{k-1} \dots\} \rightarrow \tilde{\mathbf{I}} = \{\dots I_{k+2}, -1, 0, I_{k-1} \dots\} \quad (5.9)$$

$$h_{k+1,k}^{-1} : \mathbf{I} = \{\dots I_{k+2}, 1, -1, I_{k-1} \dots\} \rightarrow \tilde{\mathbf{I}} = \{\dots I_{k+2}, 0, 0, I_{k-1} \dots\}, \quad (5.10)$$

see figures 8 and 9. We are going to show that a state with $\mathfrak{u}(1)$ charges $|J_2| < J_1$ can be mapped to the state in the Hilbert space, characterized by \mathbf{I} in the standard configuration $\mathbf{I} = \{1, 1, \dots, 1, 0, 0, \dots, 0\}$, for $J_2 \leq 0$, and $\mathbf{I} = \{-1, -1, \dots, -1, 0, 0, \dots, 0\}$ otherwise. Indeed, we can use v_k to replace all $\bar{0}$ by 0's. Next we can move magnons and anti-magnons towards each other using $r_{k+1,k}$ and $\bar{r}_{k+1,k}$ and then annihilate them in pairs using $h_{k+1,k}^{-1}$. After that, depending on the sign of J_2 there will be only magnons or anti-magnons left, which we can group together with $r_{k+1,k}$ or $\bar{r}_{k+1,k}$.

In the next section we derive what these operators correspond to in the dual description.

5.3 The fishchain reparametrization operators

Using the map between the CFT and the fishchain wavefunctions (3.21) we now map v_k^{-1} and h_k^{-1} into fishchain operators. Consider first the operator v_k^{-1} . This operator acts on a site with no magnon and maps it to a site with a magnon anti-magnon pair. Plugging it into the map (3.21) and taking into account that the conformal dimension at that site changes from $\Delta_k = 1$ to $\Delta_k = 3$, we get the equation for the corresponding operator \mathbb{V}^{-1} in AdS_5

$$v^{-1}(x) \circ \frac{1}{(Z\mathcal{X})^1} = \mathbb{V}^{-1}(Z) \circ \frac{1}{(Z\mathcal{X})^3}. \quad (5.11)$$

Using that $v^{-1}(x) = -\frac{1}{4\xi^2}\square_{\bar{x}}$ we conclude that $\mathbb{V}^{-1}(Z) = \frac{1}{2\xi^2}$, i.e. up to a multiplication by a constant this operator acts trivially in the dual picture. This is because on the fishchain side there is no real distinction between no-magnon and a magnon-anti-magnon pair at the same site, as one can see from the table 1.

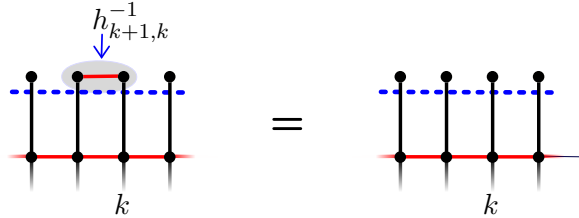


Figure 8. Graphical representation of the action of the operator $h_{k+1,k}^{-1}$, removing the ϕ_2 propagator stretched horizontally between the $k+1$ and k sites. It can be interpreted as an operator annihilating a magnon and anti-magnon situated at two neighbouring sites.

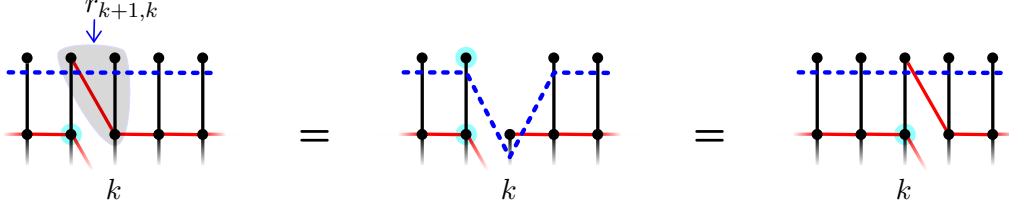


Figure 9. The operator $r_{k+1,k}$ moves a magnon at the $(k+1)$ site to the empty site on its right, (k) . Similarly, the reflection of this figure describes how the operator $\bar{r}_{k+1,k}$ moves an anti-magnon at the k 'th site to the empty site on its left $(k+1)$.

Similarly, for $h_{k+1,k}^{-1}$ (which decreases Δ_i by one on two consecutive sites) we find its AdS_5 counterpart \mathbb{H} from the following identity

$$\mathbb{H}_{\Delta_1, \Delta_2}(Z_1, Z_2) \circ \frac{1}{(Z_1 \cdot \mathcal{X}_1)^{4-\Delta_1} (Z_2 \cdot \mathcal{X}_2)^{4-\Delta_2}} = \frac{-2\mathcal{X}_1 \cdot \mathcal{X}_2}{(Z_1 \cdot \mathcal{X}_1)^{5-\Delta_1} (Z_2 \cdot \mathcal{X}_2)^{5-\Delta_2}}, \quad (5.12)$$

where Δ_j can be either 2 or 3. We find that

$$\mathbb{H}_{\Delta_1, \Delta_2}(Z_1, Z_2) = \frac{-2}{\alpha_1 \alpha_2} [\nabla_1 \cdot \nabla_2 + \alpha_1 Z_1 \cdot \nabla_2 + \alpha_2 Z_2 \cdot \nabla_1 + \alpha_1 \alpha_2 Z_1 \cdot Z_2] \quad (5.13)$$

where $\alpha_k = 4 - \Delta_k$ and⁹

$$\nabla_{j,M} = \frac{\partial}{\partial Z_j^M} + Z_j \cdot M \left(Z_j^N \frac{\partial}{\partial Z_j^N} \right). \quad (5.14)$$

As a consequence, the lift of the operator $r_{k+1,k} = h_k^{-1} \circ v_k^{-1}$, that moves a magnon to an empty site to the right reads, up to an irrelevant constant factor

$$\mathbb{H}_{3,2} = \nabla_1 \cdot \nabla_2 + 2Z_2 \cdot \nabla_1 + Z_1 \cdot \nabla_2 + 2Z_1 \cdot Z_2. \quad (5.15)$$

In the next section we will show that the *magnon move* operator $\mathbb{H}_{3,2}$ and *magnon annihilation* operator $\mathbb{H}_{2,2}$ generate a gauge symmetry of the fishchain that we interpret as discrete reparametrization symmetry.

6 Integrability, Exact Spectrum and Reparametrization Invariance

In section 4 we constructed a set of mutually commuting operators which also include the Hamiltonian \hat{H}_q . Then, in section 5, we have constructed the fishnet cut deformation operators and lifted them to fishchain operators. In this section, we use the set of commuting operators to solve for the spectrum of dimensions Δ of local operators. We then show that the cut deformation operators generate similarity transformations of the transfer matrices that can be interpreted as gauge transformations of the corresponding Baxter equation.

⁹Remember that the embedding coordinates should satisfy $Z^2 = -1$, so the ∂_Z operation is in principle not very well defined, however the combination ∇ commutes with Z^2 , making it well defined.

This section generalizes the results of [8], where the non-perturbative spectrum was obtained for the operators $J = 3$, $M = 0$ ¹⁰, and [7], where the general J , $M = 0$ case was considered. An important result of [7, 8], which we are going to use here is the *quantization condition*, which is needed in addition to the Baxter TQ-relations. We will propose the generalization of this quantization condition and also present the most general form of the TQ-relations valid for any values of the charges J_1, J_2 such that $J_1 > |J_2|$.

Using these techniques we will be able to solve numerically for several examples of states, $J = 3, M = 1$ and $J = 3, M = 2$. At finite ξ we explore a very rich analytic structure of the function $\Delta(\xi)$. At weak coupling we are able to compare our numerical results with the asymptotic Bethe ansatz, valid only up to the wrapping order $\xi^{2J+2|M|-2}$.

Our Baxter TQ-relation, which we present in this section, together with the generalization of the quantization condition of [7, 8] constitute the complete set of equations, analogous to the Quantum Spectral Curve equations for N=4 SYM [17] or ABJM [18] theory.

6.1 T-functions and Baxter TQ relation

We start by formulating the TQ-relations. In order to compare with the previous partial results of [7, 8] it is convenient to rescale the spectral parameter by ξ . To avoid confusion we denote the rescaled spectral parameter by v , which is related to the initial one by $u = v/\xi$.¹¹ We also denote by $\mathbb{T}(u)$ the eigenvalue (or T-functions) of the simultaneously diagonalizable operators $\hat{\mathbb{T}}(u)$.

The T-functions corresponding to the trivial representations can be computed explicitly

$$\mathbb{T}^1(v) = 1 \quad \text{and} \quad \mathbb{T}^{\bar{1}}(v) = \frac{v^{2J}(v+i)^{J-M+\bar{M}}(v-i)^{J+M-\bar{M}}}{\xi^{4J}}. \quad (6.1)$$

Also we notice from (4.2)-(4.4) that $\mathbb{T}^{\bar{4}}$ and \mathbb{T}^4 are closely related

$$\mathbb{T}^{\bar{4}}(v) = \frac{(-1)^J}{\xi^{2J}} (v + \frac{i}{2})^{J-M+\bar{M}} (v - \frac{i}{2})^{J+M-\bar{M}} \mathbb{T}^{4*}(-v) \quad (6.2)$$

where $*$ indicates that one should inverse the order of the particles and interchange magnons and anti-magnons. This transformation is an obvious symmetry of the system, but of course not all states are invariant under this transformation.

Baxter TQ-relations. One of the key quantities in quantum integrability are the Q-functions [19, 20]. They can be defined as T-functions corresponding to a rather complicated auxiliary space representation. As a simple alternative to defining them as eigenvalues of these complicated Q-operators, one can find them from a finite difference TQ-relation, which in our case reads¹²

$$\mathbb{T}^{1[+2]} Q^{[+4]} - \mathbb{T}^{4[+1]} Q^{[+2]} + \mathbb{T}^6 Q - \mathbb{T}^{\bar{4}[-1]} Q^{[-2]} + \mathbb{T}^{\bar{1}[-2]} Q^{[-4]} = 0. \quad (6.3)$$

¹⁰We remind that M denotes the number of magnons and \bar{M} number of anti-magnons. The $u(1)$ charges in these notations are $J_1 = J$, $J_2 = M - \bar{M}$.

¹¹When writing $\mathbb{T}(v)$, strictly speaking, what we mean is $\mathbb{T}(v/\xi)$.

¹²We use the standard shorthand notations $f^{[+a]} = f(v + \frac{ia}{2})$.

We notice that the coefficients in this equation are polynomials of different degree. However, as we can see from (6.2) even though $\mathbb{T}^{\bar{4}}(v)$ is a polynomial of degree $3J$, it has a trivial part of degree $2J$, which factorises. To remove the trivial factors we introduce the following *gauge* transformation

$$Q(v) = q(v) v^{\bar{M}} \left[\xi^{iv} e^{\frac{\pi v}{2}} \Gamma(-iv) \right]^J. \quad (6.4)$$

This transformation is designed so that the equation (6.3) becomes more symmetric

$$\begin{aligned} -\frac{P_{2J}^6(v)}{v^{J-M-\bar{M}}} q_a &= v^M (v+i)^J (v+2i)^{\bar{M}} q_a^{[+4]} - v^M (v+i)^{\bar{M}} P_J^4(v + \frac{i}{2}) q_a^{[+2]} \\ &+ v^{\bar{M}} (v-i)^J (v-2i)^M q_a^{[-4]} - v^{\bar{M}} (v-i)^M P_J^{\bar{4}}(v - \frac{i}{2}) q_a^{[-2]}, \end{aligned} \quad (6.5)$$

where we defined the degree- L polynomials P_L in the following way

$$P_J^4(v) \equiv \xi^J \mathbb{T}^4(v), \quad P_{2J}^6(v) \equiv \xi^{2J} \mathbb{T}^6(v), \quad P_J^{\bar{4}}(v) \equiv (-\xi)^J \mathbb{T}^{4*}(-v). \quad (6.6)$$

The index $a = 1, \dots, 4$ in q_a labels 4 independent solutions of (6.5). We specify below exactly how these solutions are defined by their large v asymptotic.

One can see that in the form (6.5) the Baxter TQ-equation generalizes the one derived in the CFT context in [7, 8] for the case $M = 0$. Furthermore, in [8] it is in addition assumed that the state is invariant under the inversion of the order of the sites, which we do not assume here. Our equation is thus a generalization of the results of [7, 8] to the most general states with an arbitrary number of magnons, as long as $|J_2| < |J_1|$.

Asymptotics of \mathbf{q} . The global conformal group charges Δ, S_1 and S_2 , enter into the TQ-relations through the large v asymptotic of T-functions and consequently Q-functions. Indeed, at large v the product (4.2) becomes a sum of \hat{q}_k , which is the global $\mathfrak{so}(1, 5)$ charge. This observation is reflected in the following expressions for the highest powers of the polynomials P_L :

$$\begin{aligned} P_J^4 &= v^J (\lambda_1 + \lambda_2 + \lambda_3 + \lambda_4) + \frac{v^{J-1}}{2i} [(\lambda_1 + \lambda_2 + \lambda_3 + \lambda_4)(M - \bar{M}) + \lambda_4 (\Delta - S_1 + S_2)] \\ &+ \frac{v^{J-1}}{2i} [\lambda_3 (\Delta + S_1 - S_2) + \lambda_2 (-\Delta - S_1 - S_2) + \lambda_1 (-\Delta + S_1 + S_2)] + \dots \\ P_{2J}^6 &= \left[v^{2J} + \frac{v^{2J-1}}{i} (M - \bar{M}) \right] (\lambda_1 \lambda_2 + \lambda_1 \lambda_3 + \lambda_1 \lambda_4 + \lambda_2 \lambda_3 + \lambda_2 \lambda_4 + \lambda_3 \lambda_4) \\ &- \frac{v^{2J-1}}{i} [\Delta (\lambda_1 \lambda_2 - \lambda_3 \lambda_4) + S_2 (\lambda_2 \lambda_3 - \lambda_1 \lambda_4) + S_1 (\lambda_2 \lambda_4 - \lambda_1 \lambda_3)] + \dots \\ P_J^{\bar{4}} &= v^J (\bar{\lambda}_1 + \bar{\lambda}_2 + \bar{\lambda}_3 + \bar{\lambda}_4) + \frac{v^{J-1}}{2i} [(\bar{\lambda}_1 + \bar{\lambda}_2 + \bar{\lambda}_3 + \bar{\lambda}_4)(M - \bar{M}) - \bar{\lambda}_4 (\Delta - S_1 + S_2)] \\ &- \frac{v^{J-1}}{2i} [\bar{\lambda}_3 (\Delta + S_1 - S_2) + \bar{\lambda}_2 (-\Delta - S_1 - S_2) + \bar{\lambda}_1 (-\Delta + S_1 + S_2)] + \dots \end{aligned} \quad (6.7)$$

where $\bar{\lambda}_a \equiv \frac{1}{\lambda_a}$. We remind that λ_i 's are the diagonal elements of the twist matrix G . Next, we plug the asymptotics (6.7) into the TQ-relation (6.5) to deduce the following four

possible asymptotics of the four linearly independent solutions of (6.5)

$$q_a = \lambda_a^{-iv} v^{+\mu_a - \frac{J+M+\bar{M}}{2}} + \dots, \quad \mu_a = \frac{1}{2} \begin{pmatrix} +\Delta - S_1 - S_2 \\ +\Delta + S_1 + S_2 \\ -\Delta - S_1 + S_2 \\ -\Delta + S_1 - S_2 \end{pmatrix}_a. \quad (6.8)$$

Another important asymptotic is the value of $P_{2J}^6(v)$ at the origin. Due to the relation (6.6) and the observation that $\mathbb{T}^6(0) = H_q + 1$ we have the following relation

$$P_{2J}^6(0) = \xi^{2J}. \quad (6.9)$$

This is central for how the fishchain condition $H_q = 0$ injects the information about the coupling ξ into the TQ-relations. Except for (6.9) there is no other explicit dependence on ξ appearing in (6.5).

6.2 Discrete reparametrization symmetry and integrability

The general expectation from the discrete reparametrization symmetry, described in section 3.3, is that the spectrum and other integrals of motion should remain invariant. In this section we will prove this is indeed the case based on the integrability construction described in the previous section.

Magnon reordering symmetry. One can immediately notice that the Baxter equation (6.5) does not contain any explicit reference to the ordering of the particles. The equation only depends on the number of magnons M and anti-magnons \bar{M} , but not on their particular ordering along the fishchain. Furthermore, we will see below that the Baxter TQ-relations depends non-trivially only on the difference $J_2 = M - \bar{M}$.

At the level of the eigenvector this symmetry is less obvious. In section 3.3 we have shown that wave functions with different magnon positions corresponds to different ways of cutting the same Feynman diagrams. Using this picture, we have argued that a shift in the magnon position should be thought of as a discrete reparametrization symmetry of the fishchain model. This shift is generated by the fishchain operator $\mathbb{H}_{3,2}$ in (5.15). We will now prove that indeed, this operator generates a symmetry of the transfer matrix.

$$\mathcal{R}_{21} \equiv \mathbb{H}_{3,2}(Z_1, Z_2) = \nabla_1 \cdot \nabla_2 + \nabla_2 \cdot Z_1 + 2Z_2 \cdot \nabla_1 + 2Z_1 \cdot Z_2. \quad (6.10)$$

The operator \mathcal{R}_{21} has the following key property

$$\begin{aligned} & \mathbb{L}_2^{ab}(u) \mathbb{L}_1^{bc} \left(u - \frac{i}{2\xi} \right) \mathcal{R}_{21} - \mathcal{R}_{21} \mathbb{L}_2^{ab} \left(u - \frac{i}{2\xi} \right) \mathbb{L}_1^{bc}(u) \\ &= \frac{i \Sigma_{NM}^{ac}}{2\xi^2} \left[(Z_2^N \nabla_1^M + Z_2^N Z_1^M) \left(\frac{\xi^2 \text{tr } q_2^2}{2} - 4 \right) - (Z_1^N \nabla_2^M + 2Z_1^N Z_2^M) \left(\frac{\xi^2 \text{tr } q_1^2}{2} - 3 \right) \right]. \end{aligned} \quad (6.11)$$

At first sight it looks quite complicated, however, one can see easily that on the states with a magnon on site 1 and no magnon on 2 the r.h.s. become zero and the operator \mathcal{R} become the interchange operator which exchanges the roles between the magnons and no-magnons.

The existence of such operators guarantees that the spectrum of all integrals of motion does not depend on the initial order of the magnons. This ensures the self-consistency of our approach.

More precisely we can see that the magnon move operation results in the following similarity transformation

$$\hat{\mathbb{T}}^{\mathbf{I}}(u) |\Psi\rangle^{\mathbf{I}} = (\mathcal{R}_{k,k+1})^{-1} \hat{\mathbb{T}}^{\leftrightarrow \mathbf{I}}(u) \mathcal{R}_{k,k+1} |\Psi\rangle^{\mathbf{I}} = (\mathcal{R}_{k,k+1})^{-1} \hat{\mathbb{T}}^{\leftrightarrow \mathbf{I}}(u) |\Psi\rangle^{\leftrightarrow \mathbf{I}} \quad (6.12)$$

where the set \mathbf{I} is such that $I_k = 1$ and $I_{k+1} = 0$, whereas the transformed set $\leftrightarrow \mathbf{I}$ corresponds to the magnon at $k+1$ i.e. $I_k = 0$ and $I_{k+1} = 1$. The equation (6.12) ensures that the spectrum of all conserved charges before and after the magnon move operation stays unchanged. Similarly, we can shift an anti-magnon to the left and all conserved charges are unaffected.

Magnon–anti-magnon annihilation. First, let us demonstrate that the spectrum does not change when we simultaneously remove one magnon and one anti-magnon. We will establish a simple relation between the solutions of the Baxter equation with different numbers of magnons. Consider the transformation $M \rightarrow M - n$, $\bar{M} \rightarrow \bar{M} - n$. Under this transformation (6.5) becomes

$$\begin{aligned} -\frac{P_{2J}^6(v)}{v^{J-M-\bar{M}+2n}} \tilde{q}_a &= \frac{v^M(v+i)^J(v+2i)^{\bar{M}}}{v^n(v+2i)^n} \tilde{q}_a^{[+4]} - \frac{v^M(v+i)^{\bar{M}}}{v^n(v+i)^n} P_J^4(v+\frac{i}{2}) \tilde{q}_a^{[+2]} \\ &+ \frac{v^{\bar{M}}(v-i)^J(v-2i)^M}{v^n(v-2i)^n} \tilde{q}_a^{[-4]} - \frac{v^{\bar{M}}(v-i)^M}{v^n(v-i)^n} P_J^4(v-\frac{i}{2}) \tilde{q}_a^{[-2]}. \end{aligned} \quad (6.13)$$

First we see that the overall factor $1/v^n$ cancels. Furthermore, by denoting $q(v) = \frac{\tilde{q}(v)}{v^n}$ we return back to the initial form (6.5).

At the level of the fishchain wave function, we can always shift the positions of the magnon and anti-magnon until the anti-magnon is at the first site and the magnon is at the second site. To Annihilate them, we act with

$$\mathbb{H}_{2,2}(Z_1, Z_2) \propto \tilde{\mathcal{R}}_{12} = \nabla_1 \cdot \nabla_2 + 2Z_2 \cdot \nabla_1 + 2Z_1 \cdot \nabla_2 + 4Z_1 \cdot Z_2. \quad (6.14)$$

This operator has the following property

$$\begin{aligned} &\mathbb{L}_1^{ab}(u) \mathbb{L}_2^{bc}(u) \tilde{\mathcal{R}}_{12} - \tilde{\mathcal{R}}_{12} \mathbb{L}_1^{ab}(u - \frac{i}{2\xi}) \mathbb{L}_2^{bc}(u + \frac{i}{2\xi}) \\ &= \frac{i \Sigma_{NM}^{ac}}{2\xi^2} \left[(Z_1^N \mathcal{D}_2^M + 2Z_1^N Z_2^M) \left(\frac{\xi^2 \text{tr } q_1^2}{2} - 4 \right) - (Z_2^N \mathcal{D}_1^M + 2Z_2^N Z_1^M) \left(\frac{\xi^2 \text{tr } q_2^2}{2} - 4 \right) \right]. \end{aligned} \quad (6.15)$$

Similar to (6.11) the r.h.s. of the above equation vanishes on the states with magnon and anti-magnon. This relation leads to an analog of (6.12) where the initial set \mathbf{I} has $I_{k+1} = 1$ and $I_k = -1$, whereas the resulting set $\leftrightarrow \mathbf{I}$ has no magnons at these positions i.e. $\leftrightarrow I_k = \leftrightarrow I_{k+1} = 0$. We see again that the magnon annihilation operation does not affect the spectrum of any of the the conserved charges.

6.3 Quantization condition and exact spectrum

In order to adapt the quantization condition of [7] to the general case with any number of magnons, we introduce two sets of solutions of the TQ-relations (6.5). One set, denoted by $q_a^\downarrow(v)$, is regular in the upper half-plane and satisfy (6.8) at large v . The other set, $q_a^\uparrow(v)$, is regular in the lower half-plane. It is easy to see that such solutions exist and that they can be constructed numerically, using the methods of [21].

Since there are only 4 independent solutions of the 4th order finite difference equation (6.5), these two sets $q_a^\downarrow(v)$ and $q_a^\uparrow(v)$ should be linearly dependent with i -periodic coefficients, i.e.

$$q_a^\uparrow(v) = \Omega_a^b(v) q_b^\downarrow(v) , \quad \Omega_a^b(v+i) = \Omega_a^b(v) . \quad (6.16)$$

The matrix $\Omega_a^b(v)$ itself can be constructed from q -functions as the simple ratio of two determinants

$$\Omega_a^b(v) = \frac{\epsilon^{b b_1 b_2 b_3}}{3!} \frac{\det_{n=0,\dots,3} \{q_a^\uparrow(v-in), q_{b_1}^\downarrow(v-in), q_{b_2}^\downarrow(v-in), q_{b_3}^\downarrow(v-in)\}}{\det_{n=0,\dots,3} \{q_1^\downarrow(v-in), q_2^\downarrow(v-in), q_3^\downarrow(v-in), q_4^\downarrow(v-in)\}} , \quad (6.17)$$

as follows from (6.16).

In [7] it is shown that this matrix $\Omega_a^b(v)$ should satisfy the following *quantization condition*¹³

$$\Omega_1^2 = \Omega_2^1 = \Omega_3^4 = \Omega_4^3 = 0 , \quad (6.18)$$

which singles out physical solutions of the TQ-relations. Furthermore, one can show [7] that the i -periodic function $\Omega_a^b(u)$ has simple poles at $u = in$ of order J . This implies that each matrix element of $\Omega_a^b(u)$ can be parametrized by $J+1$ constants $C^{(n)}$ as

$$\Omega_a^b(u) = \frac{\sum_{n=0}^J C^{(n)}{}_a^b e^{2\pi n u}}{(1 - e^{2\pi u})^J} , \quad (6.19)$$

where in addition for off-diagonal elements only J constants $C^{(n)}$ are non-zero. This implies that we have $4J$ equations in (6.18). One can show that only $4J-3$ of these conditions are linearly independent (for large enough J), which is exactly how many free parameters we have in the polynomial coefficients P_L in (6.5). Thus, using the quantization condition (6.18) we should be able to fix all coefficients in the Baxter TQ-relations, which also includes Δ .

In the next section we report on the numerical tests of this procedure for the case with magnons.

6.4 Numerical tests

In this section we apply the procedure described in section 6.3 for two cases, $J=3$, $M=1$ and $J=3$, $M=2$. In order to solve the Baxter TQ-relations (6.5) we use the method of [8, 21]. Then we use the generalized gluing conditions (6.18) to fix the parameters in

¹³We are grateful to the authors of [7] for sharing this unpublished result with us

(6.5). In both cases we found perfect agreement with the Asymptotic Bethe Ansatz (ABA) of [9, 10] at weak coupling. In this section we fix the twist parameters as $\lambda_1 = e^{i/3}$, $\lambda_2 = e^{-i/3}$, $\lambda_3 = e^{i/2}$, $\lambda_4 = e^{-i/2}$.

6.4.1 Length three, one magnon

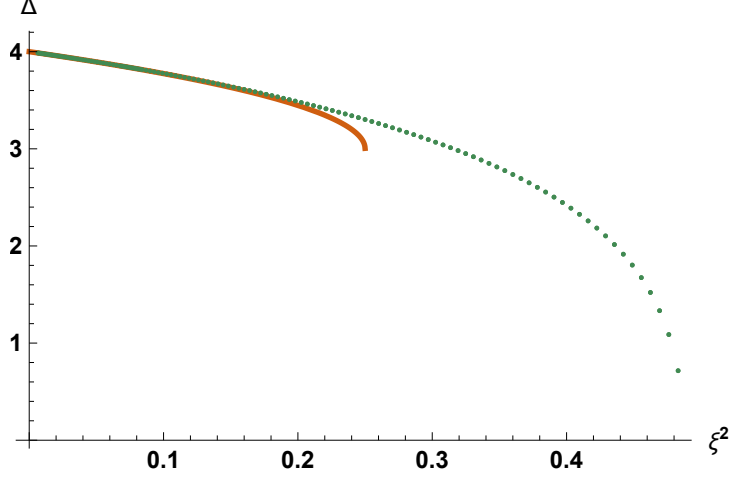


Figure 10. Numerical solution (dots) and the Asymptotic Bethe Ansatz prediction (solid line) match perfectly at small coupling for the state with one magnon and $J = 3$. The two start to deviate from each other at larger values of ξ^2 .

We generated to a very high precision numerical values for a wide range of couplings using the method described in 6.3 (see figure 10). In order to check our results we have to recall that in the ABA approach for one magnon one only needs to know the *dispersion relation* $\Delta_{ABA} = J + \sqrt{1 - 4\xi^2}$, which is expected to be accurate up to the wrapping order $\xi^{2J+2M} = \xi^8$.

Indeed, by making a fit of our numerical values with even powers of ξ we found the following expansion

$$\Delta_{TQ} = 4. - 2.\xi^2 - 2.\xi^4 - 4.\xi^6 + 0.155845\xi^8 + \dots \quad (6.20)$$

We see that the first 4 coefficients are integers, and agree precisely with the magnon dispersion relation. At order ξ^8 we get some real number, which is expected to be a combination of two polylogarithms Li_3 and Li_5 with the arguments depending on the twists.

What is very interesting is the analytic structure of our result in ξ . At small enough ξ the function has a regular (convergent) expansion in powers of ξ^2 . At $\xi \sim 0.7$ the dimension Δ tends to 0 and after that point become purely imaginary (see figure 10). The value $\xi \sim 0.7$ is thus a branch point. This is not the only branch cut of the function $\Delta(\xi)$. The function $\Delta(\xi)$ is in fact a multivalued function with infinitely many sheets (see figure 11), containing not just one but infinitely many local operators, which can be identified at weak coupling as $\text{tr } \phi_1^3 \phi_2 (\phi_2 \phi_2^\dagger)^n$ (up to permutations).

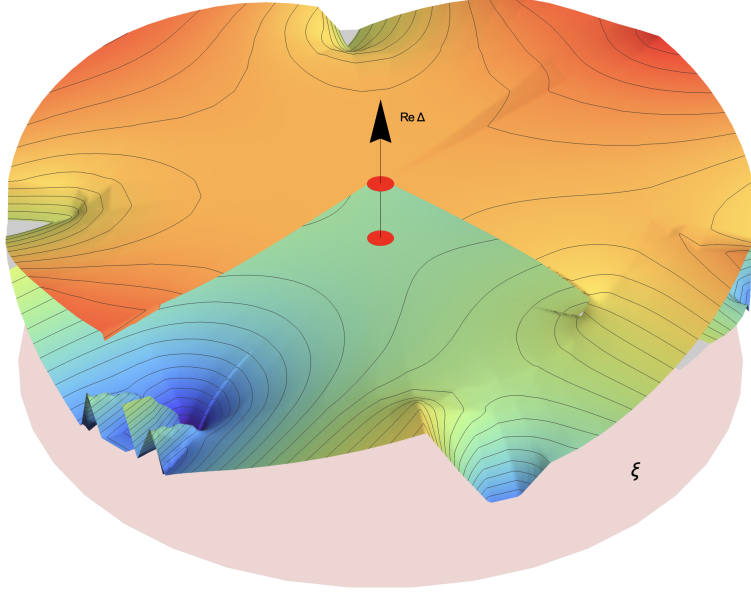


Figure 11. Single magnon operator $\text{tr } \phi_1^2 \phi_2$ has a dimension Δ , which is a multivalued function of ξ . At weak coupling the bare dimension of the state is $J_1 + J_2 = 4$. Analytically continuing in ξ one can discover an infinite tower of states with the bare dimensions $4 + 2n$, $n = 0, 1, \dots$ ($n = 0, 1$ are indicated by the red dots on the picture).

6.4.2 Length three, two magnons

We also found a numerical solution in the two magnon case for the chain of length $J = 3$. Again our results are in complete agreement with the ABA prediction at weak coupling. Note that this time, the ABA calculation involves a rather non-trivial dressing phase, which gives rise to the ζ values in the result

$$\begin{aligned} \Delta_{ABA} = & 5 + \left(\sqrt{5} - 1\right) \xi^2 + \left(\frac{3}{\sqrt{5}} - 1\right) \xi^4 - \left(2 + \frac{2}{5\sqrt{5}}\right) \xi^6 \\ & + \left(-\frac{4\zeta_3}{\sqrt{5}} - 4\zeta_3 + \frac{81}{25\sqrt{5}} + 3\right) \xi^8 + \left(\frac{112\zeta_3}{5\sqrt{5}} - \frac{424}{25\sqrt{5}} + 8\right) \xi^{10} + \mathcal{O}(\xi^{12}) . \end{aligned} \quad (6.21)$$

Our numerical fit of the result of solution of the TQ-relations gives

$$\Delta_{TQ} = 5 + 1.23607\xi^2 + 0.341641\xi^4 - 2.17889\xi^6 - 2.50956\xi^8 - 0.575805\xi^{10} + \dots \quad (6.22)$$

which agrees perfectly with the first 4-loops predicted by ABA (6.21). At the wrapping order $\xi^{2J+2M} = \xi^{10}$, as expected, the ABA result is no longer valid and deviates from our numerical prediction (6.22).

In conclusion, the fact that we managed to reproduce the ABA prediction from the TQ-relations provides a very non-trivial test of our approach.

7 Conclusion

In this paper, we completed the derivation of the Holographic dual of the fishnet theory. Introducing the magnons, i.e. ϕ_2 and/or ϕ_2^\dagger fields, into the consideration brought some

surprises. Firstly, we found that the classical limit $\xi \rightarrow \infty$ remain unchanged. Namely, we still find the same classically integrable fishchain model, which is a classical chain of particles on a light-cone with nearest-neighbor interaction. The essence of the magnons is hiding in the details of the quantization procedure, which also modifies the light-cone into the AdS_5 space. This is, in fact, in complete agreement with the exact spectrum and 4-point function computation in [13] for the length-two operators. Secondly, the introduction of the magnons revealed a new nice feature, namely the *discrete reparametrization symmetry* – an invariance of the physics w.r.t. different sectioning of the discretized world-sheet of the fishchain into space-like slices. The magnons in this picture indicate bends of the curve cutting the world-sheet. Mathematically this symmetry manifests as a map between Hilbert spaces, preserving the integrability and conserved charges that uniquely characterize the state.

Another important output of our analysis is the universal integrability picture, which includes all possible insertions on equal footing. We found the quantum Baxter TQ-relations, which together with the quantization condition [7, 8], give us direct access to the quantum spectrum of the model in complete generality.¹⁴ This also opens ways to the separation of variables (SoV) construction, along the lines of the recent works [22–25].

Among open questions remains a particular configuration when the number of magnons saturates the number of states, i.e. when both $u(1)$ charges are equal $|J_1| = |J_2|$. In this case, surprisingly, the general strategy outlined in this paper fails. On some particular examples it is known that this case produces a more complicated result for the spectrum even for short operators, tractable with the conformal symmetry alone [13]. Nevertheless, the integrability should be present in this case too [7], but the strong coupling behavior is very different, indicating that it is mysteriously missing in the current picture. This problem could be related to another large part of states which happened to be protected, and decoupled from the dynamical part of the spectrum studied in this paper. The reason why there is a large number of states with protected dimension is also unclear, there is no manifest symmetry, like supersymmetry, which can help to explain this phenomenon.

Acknowledgements

We thank O. Aharony, D. Grabner, V. Kazakov, G. Korchemsky and A. Zhiboedov for invaluable discussions. We thank J. McGovern for comments on the manuscript. N.G. was supported by the STFC grant (ST/P000258/1). A.S. was supported by the I-CORE Program of the Planning and Budgeting Committee, The Israel Science Foundation (1937/12).

References

- [1] Ö. Gürdoğan and V. Kazakov, “New Integrable 4D Quantum Field Theories from Strongly Deformed Planar $\mathcal{N} = 4$ Supersymmetric Yang-Mills Theory,” Phys. Rev. Lett. **117**, no. 20, 201602 (2016) Addendum: [Phys. Rev. Lett. **117**, no. 25, 259903 (2016)] doi:10.1103/PhysRevLett.117.201602, 10.1103/PhysRevLett.117.259903 [arXiv:1512.06704 [hep-th]].

¹⁴This spectrum was previously only available for a rather narrow subset of states [8].

- [2] H. B. Nielsen and P. Olesen, “A Parton view on dual amplitudes,” *Phys. Lett.* **32B**, 203 (1970). doi:10.1016/0370-2693(70)90474-0
- [3] A. B. Zamolodchikov, “‘fishnet’ Diagrams As A Completely Integrable System,” *Phys. Lett.* **97B**, 63 (1980). doi:10.1016/0370-2693(80)90547-X
- [4] N. Gromov and A. Sever, “The Holographic Fishchain,” *Phys. Rev. Lett.* **123** (2019) 081602 doi:10.1103/PhysRevLett.123.081602 [arXiv:1903.10508 [hep-th]].
- [5] N. Gromov and A. Sever, “Quantum Fishchain in AdS_5 ,” arXiv:1907.01001 [hep-th].
- [6] D. Chicherin, V. Kazakov, F. Loebbert, D. Muller and D. I. Zhong, “Yangian Symmetry for Fishnet Feynman Graphs,” *Phys. Rev. D* **96**, no. 12, 121901 (2017) doi:10.1103/PhysRevD.96.121901 [arXiv:1708.00007 [hep-th]].
- [7] D. Grabner, N. Gromov, V. Kazakov, G. Korchemsky, in preparation.
- [8] N. Gromov, V. Kazakov, G. Korchemsky, S. Negro and G. Sizov, “Integrability of Conformal Fishnet Theory,” arXiv:1706.04167 [hep-th].
- [9] J. Caetano, Ö. Gürdoğan and V. Kazakov, “Chiral limit of $\mathcal{N} = 4$ SYM and ABJM and integrable Feynman graphs,” *JHEP* **1803**, 077 (2018) doi:10.1007/JHEP03(2018)077 [arXiv:1612.05895 [hep-th]].
- [10] A. C. Ipsen, M. Staudacher and L. Zippelius, “The one-loop spectral problem of strongly twisted $\mathcal{N} = 4$ Super Yang-Mills theory,” *JHEP* **1904**, 044 (2019) doi:10.1007/JHEP04(2019)044 [arXiv:1812.08794 [hep-th]].
- [11] J. Fokken, C. Sieg and M. Wilhelm, “Non-conformality of γ_i -deformed $N = 4$ SYM theory,” *J. Phys. A* **47** (2014) 455401 doi:10.1088/1751-8113/47/45/455401 [arXiv:1308.4420 [hep-th]].
- [12] C. Sieg and M. Wilhelm, “On a CFT limit of planar γ_i -deformed $\mathcal{N} = 4$ SYM theory,” *Phys. Lett. B* **756**, 118 (2016) doi:10.1016/j.physletb.2016.03.004 [arXiv:1602.05817 [hep-th]].
- [13] N. Gromov, V. Kazakov and G. Korchemsky, “Exact Correlation Functions in Conformal Fishnet Theory,” arXiv:1808.02688 [hep-th].
- [14] P. A. M. Dirac, “Wave equations in conformal space,” *Annals Math.* **37**, 429 (1936). doi:10.2307/1968455
- [15] D. Simmons-Duffin, “Projectors, Shadows, and Conformal Blocks,” *JHEP* **1404**, 146 (2014) doi:10.1007/JHEP04(2014)146 [arXiv:1204.3894 [hep-th]].
- [16] A. Cavaglià, D. Grabner, N. Gromov and A. Sever, To appear.
- [17] N. Gromov, V. Kazakov, S. Leurent and D. Volin, “Quantum Spectral Curve for Planar $\mathcal{N} = 4$ Super-Yang-Mills Theory,” *Phys. Rev. Lett.* **112** (2014) no.1, 011602 doi:10.1103/PhysRevLett.112.011602 [arXiv:1305.1939 [hep-th]].
- [18] A. Cavaglià, D. Fioravanti, N. Gromov and R. Tateo, “Quantum Spectral Curve of the $\mathcal{N} = 6$ Supersymmetric Chern-Simons Theory,” *Phys. Rev. Lett.* **113** (2014) no.2, 021601 doi:10.1103/PhysRevLett.113.021601 [arXiv:1403.1859 [hep-th]].
- [19] R. J. Baxter, “Eight vertex model in lattice statistics and one-dimensional anisotropic Heisenberg chain. 1. Some fundamental eigenvectors,” *Annals Phys.* **76**, 1 (1973). doi:10.1016/0003-4916(73)90439-9
- [20] V. V. Bazhanov, S. L. Lukyanov and A. B. Zamolodchikov, “Integrable structure of conformal field theory. 2. Q operator and DDV equation,” *Commun. Math. Phys.* **190** (1997) 247 doi:10.1007/s002200050240 [hep-th/9604044].

- [21] N. Gromov, F. Levkovich-Maslyuk and G. Sizov, “Quantum Spectral Curve and the Numerical Solution of the Spectral Problem in AdS5/CFT4,” JHEP **1606** (2016) 036 doi:10.1007/JHEP06(2016)036 [arXiv:1504.06640 [hep-th]].
- [22] N. Gromov, F. Levkovich-Maslyuk and G. Sizov, “New Construction of Eigenstates and Separation of Variables for SU(N) Quantum Spin Chains,” JHEP **1709** (2017) 111 doi:10.1007/JHEP09(2017)111 [arXiv:1610.08032 [hep-th]].
- [23] P. Ryan and D. Volin, “Separated variables and wave functions for rational gl(N) spin chains in the companion twist frame,” J. Math. Phys. **60** (2019) no.3, 032701 doi:10.1063/1.5085387 [arXiv:1810.10996 [math-ph]].
- [24] S. Derkachov, V. Kazakov and E. Olivucci, “Basso-Dixon Correlators in Two-Dimensional Fishnet CFT,” JHEP **1904** (2019) 032 doi:10.1007/JHEP04(2019)032 [arXiv:1811.10623 [hep-th]].
- [25] A. Cavaglià, N. Gromov and F. Levkovich-Maslyuk, “Separation of variables and scalar products at any rank,” arXiv:1907.03788 [hep-th].
- [26] N. Beisert, B. Eden and M. Staudacher, “Transcendentality and Crossing,” J. Stat. Mech. **0701**, P01021 (2007) doi:10.1088/1742-5468/2007/01/P01021 [hep-th/0610251].